의학박사 학위논문

당뇨병성 신증모델에서 항노화물질인 αklotho의 신기능 보호 효과

2021년 2월

서울대학교 대학원

의학과 중개의학

이 진 호

당뇨병성 신증모델에서 항노화물질인 αklotho의 신기능 보호 효과

지도 교수 강 희 경

이 논문을 의학박사 학위논문으로 제출함
2020년 10월

서울대학교 대학원
의학과 중개의학전공
이 진 호

이진호의 의학박사 학위논문을 인준함
2021년 1 월

위 원 장 오 국 환 (인)

부위원장 강 희 경 (인)

위 원 조 영 민 (인)

위 원 유 태 현 (인)

위 원 한 승 석 (인)

Abstract

Renal protective effects of αklotho in diabetic nephropathy model

- αklotho on diabetic nephropathy -

Jinho Lee

Department of Translational Medicine

The Graduate School

Seoul National University

αklotho is an anti-ageing protein mainly expressed in the kidney. αklotho exists as two different forms, membrane and soluble αklotho, and soluble αklotho enters into the circulation. αklotho mainly functions as co-receptor of fibroblast growth factor 23 (FGF23) and causes phosphaturia. However, αklotho has various effects including autophagy, wound healing, insulin sensitivity, and calcium homeostasis and to have

anti-fibrosis, antioxidant, and anti-senescence activity, suggesting that αklotho functions beyond FGF23 signaling. In fact, studies reported that inducing *klotho* expression or treating αklotho protein are resulted as renal protective effects. Since αklotho declines during renal dysfunction, including diabetic nephropathy (DN), we hypothesized that αklotho may perform renal protective effects against DN. To find out, recombinant αklotho protein was injected to db/db mice, which is type 2 diabetes mouse model. As result, αklotho protected podocytes by suppressing DN-induced TRPC6 overexpression. Moreover, αklotho is discovered to have mitochondrial protective roles in proximal tubule, by activating AMPK-PGC1α signaling. In addition, in distal tubule, αklotho enhanced TRPV5 calcium transporter, therefore ameliorates hypocalcinuria, which is an early symptom of DN. Taken together, αklotho shows renal protective effects against DN in various renal cells.

Part of the results in this thesis have been published in the following paper:

Lee, J., et al. (2020). "Klotho ameliorates diabetic nephropathy via

LKB1-AMPK-PGC1α-mediated renal mitochondrial protection". Biochem BioPhys Res Commun

Keywords: αklotho, Diabetic nephropathy (DN), podocytes, Transient receptor potential canonical 6 (TRPC6), proximal tubule, mitochondria, adenosine monophosphate-activated protein kinase (AMPK), Peroxisome proliferator-activated receptor gamma coactivator 1-alpha (PGC1α), distal tubule, transient receptor potential vanilloid type 5 (TRPV5), galectin 1.

Student Number: 2016-20030

Table of Contents

Chapter 1. General Information

1.1 Background

Diabetes is a disease that causes excessive blood glucose, and it is closely related to chronic kidney disease (CKD) and aging. About half of type 2 diabetes (T2D) and one-third of type 1 diabetes (T1D) patients show renal dysfunction or albuminuria[1,2]. Therefore, diabetic nephropathy (DN) is a major cause of end stage renal disease (ESRD) in the United States[3].

αKlotho was first identified as an antiaging protein. αKlotho is a type 1 transmembrane protein expressed mainly in the kidney[4]. In the kidney, αKlotho expression is highest in the distal tubule, though it also occurs in the proximal tubule (PT) and podocytes. In the PT, αKlotho is best known as a co-receptor for fibroblast growth factor 23 (FGF23)[5] and induces phosphaturia by suppressing sodium phosphorous co-transporter 2[6]. The extracellular domain of αKlotho can be cleaved by secretases[7,8]. Cleaved αKlotho is released into the circulation as soluble αKlotho and affects multiple organs[9,10] beyond FGF23 signaling. Recent studies analyzing the structures of αKlotho and βKlotho revealed that they have

a specific receptor binding arm (RBA) domain. The RBA is pivotal for binding with FGF receptor 1 (FGFR1) and is unstructured unless it interacts with its target. Such proteins are called *intrinsically disordered*, and they can interact with various proteins. Thus, αKlotho certainly has FGF23-independent roles[11,12]. So far, αKlotho is known to stimulate autophagy, wound healing, insulin sensitivity, and calcium homeostasis and to have anti-fibrosis, antioxidant, and anti-senescence activity[13,14].

1.2. Purpose of Research

Three experimental studies (Chapter 2, 3, and 4) were designed in order to demonstrate the renal protective effects of αklotho against DN. The first study (Chapter 2) was to find out whether αklotho protects podocytes from DN-induced cell damage, by suppressing TRPC6 overexpression on podocytes. TRPC6 is a calcium transporter causes calcium uptake, and its overexpression causes increased intracellular calcium concentration in podocytes, results in podocyte damage.

The second study (Chapter 3) was to define that αklotho protects mitochondria in renal proximal tubule by activating AMPK-PGC1α pathway. Mitochondrial dysfunction caused by oxidative stress is one of the main causes of cellular damage during diabetes, and *KLOTHO* knock out mice showed serious mitochondrial dysfunction. The study was to find out whether αklotho has anti-diabetic effects by showing renal mitochondrial protective effects.

The purpose of the last study (chapter 4) was to discover the mechanism how soluble αklotho increases TRPV5 calcium transporter on distal tubule membrane. Previously, soluble αklotho was known to ameliorate hypocalcinuria by increasing TRPV5 on renal distal tubule, by cleaving α2-3-sialyllactose of TRPV5, causes it to bind with membrane protein galectin-1, thereby holding it on the membrane. However, recent study discovered that soluble αklotho actually binds to α2-3-sialyllactose, rather than cleaving, so the mechanism how soluble αklotho increases TRPV5 was back to elusive. The study hypothesized that soluble αklotho binds to both TRPV5 and galectin-1, therefore functions as bridge that anchors TRPV5 on the membrane.

Chapter 2. Klotho ameliorates diabetic nephropathy by suppressing TRPC6 in podocytes

2.1 Background

Diabetic nephropathy (DN) is the leading cause of end-stage-renal disease (ESRD)[1]. An early manifestation of DN is albuminuria, and it is due to the damage of glomerular filtration barrier. Podocytes are terminally differentiated epithelial cells which maintains glomerular filtration barrier. Podocyte injury directly leads to damage of glomerular filtration barrier, and it is closely related to many glomerular diseases, including DN[15]. Therefore, protecting podocytes from diabetes-mediated injury is important in the prevention and treatment of DN.

Currently, therapies against DN are targeting renin-angiotensin system (RAS). Inhibiting RAS reduces blood pressure, decreases albuminuria, and delays renal fibrosis. Angiotensin II (Ang II) is one of molecules activated by RAS, and activated Ang II is shown to have negative effects on the podocytes, including abnormal podocyte Ca^2 signaling[16-18] and reactive

oxygen species (ROS) production[19]. Increased levels of Ang II have been found in the diabetic kidney.

Transient receptor potential canonical 6 (TRPC6) is a calcium channel that promotes calcium intake into podocytes. An important link between abnormal intracellular calcium and podocyte injury is the finding that increased TRPC6 by phosphatidylinositol 3-kinases (PI3K) mediated exocytosis, or Ang II-Nox4 mediated oxidative stress mediates over influx of calcium into podocytes. Such enhanced intracellular calcium activates the Ca^2 dependent phosphatase, calcineurin, which cleaves synaptopodin by cathepsin L, and results in podocyte injury and proteinuria. Activation of calcineurin in podocytes alone is proven sufficient to cause degradation of synaptopodin, podocyte injury, and proteinuria[20]. In addition, gain-of-function mutation in TRPC6 caused focal segmental glomerulosclerosis (FSGS)[21-23], and enhanced TRPC6 is associated with proteinuric kidney disease[24]. The calcineurin inhibitor, cyclosporine A (CsA), prevents synaptopodin degradation *in vitro*, and mice resistant to cathepsin-mediated synaptopodin degradation are protected from proteinuria[20]. Therefore, preventing TRPC6 overexpression is important

for protecting podocytes, and αklotho is reported to suppress TRPC6 from podocytes in a murine model of chronic kidney disease (CKD) by inhibiting PI3K. Moreover, TRPC6 transgenic mice showed albuminuria resulted in ameliorated urine albumin by treating recombinant α-klotho protein (rKL)[25].

DN is featured with enhanced TRPC6 expression on podocytes through Ang II, RAS, NOX4, and ROS, resulting in the podocyte injury and albuminuria[26]. While α-klotho is known to suppress TRPC6 expression by inhibiting PI3K-mediated exocytosis in nephrectomy mice[27], whether αklotho inhibits TRPC6 by suppressing NOX4 in DN is unknown. Since α-klotho is an anti-ageing molecule that reduces oxidative stress by activating cAMP/protein kinase A (PKA) pathway[28], we hypothesized that treating rKL into db/db mice would protect podocyte by suppressing TRPC6 expression in diabetic nephropathy.

2.2 Materials and Methods

2.2.1. Animals

Animal experiments were performed with the approval of the Institutional Animal Care and Use Committee of Seoul National University Hospital (IACUC 15-0055-C1A0). Six-week old male db/db mice (C57BL/6 background) were used in this study. db/m mice were used as control. All mice were purchased from OrientBio (Seong-Nam, Korea). Baseline data were collected immediately after arrival, and mice were given 10 days for adaptation. After that, mice were injected intraperitoneally with either rKL (R&D SYSTEMS, Ala35-Lys982, 10μg/kg) in saline or vehicle. The injection was given every day for 8 weeks. Three or four mice were housed per cage. They were kept in 12h light and 12h dark cycle. 24h urine was collected using metabolic cage without food supply at fourth and eighth week. Final data was recorded at the eighth week just before sacrifice. One kidney from each mouse was fixed in 4% paraformaldehyde and then embedded in paraffin for histologic analysis, and the other kidney was used for western blot analysis.

2.2.2. Cell culture

Mouse podocytes were proliferated and differentiated in different condition as previously reported[29]. Before seeding, plates were coated with fibronectin. For proliferation, cells were incubated in RPMI1640 (Gibco) containing 10% fetal bovine serum (FBS, Gibco), with interferon-γ, and in 33℃. After reaching 80% confluence of the culture dish, we set a different condition to induce cell differentiation. For differentiation, cells were incubated in RPMI1640 containing 5% FBS, without interferon-γ, and in 37℃, for 72 hours. After that, cells were starved by culturing in RPMI1640 without FBS for 24 hours before treating glucose and rKL. 30mM D-glucose was given for high glucose (HG) condition, and 5mM D-glucose for normal glucose (NG). 10nM of rKL was treated for 24h.

2.2.3. Western Blotting

Proteins from mouse kidneys and cultured cells were extracted using RIPA lysis buffer. The following primary antibodies were used: TRPC6 (Alomone Labs ACC-017), α-klotho (sc 22220), NOX4 (sc-21860), PI3K (ab 86714), NF- B (sc-33020), calcineurin (ab 3763), prohibitin 2 (Bio Legend 603102), synaptopodin (ab224491), and Klf 6 (sc-365633). Forty micrograms of proteins were loaded into each lane, and 4~16% gradient SDS-PAGE were used. Proteins were transferred onto nitrocellulose membranes (Amersham, Arlington Heights, IL).

2.2.4 Renal ROS measurement

Sliced renal cortex tissue was incubated in 20μM DCF-DA (ab 65319) in PBS at 37℃ for 45 min. After incubation, the samples were washed using PBS. The samples were then read at Ex485nm/Em535nm using confocal microscopy (x200, Leica).

2.2.5 Immunofluorescence

Primary antibodies were used as follows: TRPC6 (Alomone Labs ACC-017, 1:100) and synaptopodin (ab224491, 1:500).

Secondary antibodies were used as follows: Goat Anti-Rabbit IgG Alexa Fluor 488 (ab150077, 1:2000), and Donkey Anti-Rabbit IgG Alexa Fluor 647 (ab150075, 1:2000). Cells were treated with DAPI (Carl Roth, 6843.1, 1:2000) to stain the nucleus.

2.2.6 Transmission Electron Microscopy (TEM)

Pieces of renal cortex tissue were first fixed in 4% paraformaldehyde, then fixed in 1% osmium tetroxide, dehydrated by treating graded alcohols, and embedded in Epon. Ultrathin sections (200–400 Å) were cut on nickel grids, stained with uranyl acetate, and observed at x12,000 using a digital electron microscope (JEM-1400; JEOL Ltd.).

2.2.7 MTT analysis

$1X10^3$ podocytes were seeded on each well in 96 well plate. Number of live cells were analyzed using MTT assay kit (ab 211091). Proliferation, differentiation and glucose treatment were processed as described in above (2.2 Cell culture). After treating NG or HG for 24h, we replaced to starvation media with rKL and MTT reagent in cell cultures. We incubated the plate for 3 hr at 37°C, and added MTT solvent and incubated for 15 min. The plate was read at 590 nm using a microplate reader (Molecular Devices, San Jose, CA) to analyze the number of live cells.

2.2.8 Intracellular calcium measurement

Intracellular calcium concentration of cultured mouse podocyte was measured by using Calcium Colorimetric Assay Kit (Biovision K380). Samples were prepared as podocyte cell lysate treated with NG or HG, and with or without rKL. $3 X 10^4$ cells were lysated from each group, and

the lysate was diluted with H_2O to set the final sample volume to 150μl. 50μl of each sample was added into each well in 96-well plate, to define statistical significance. 90 μl of the Chromogenic Reagent and 60 μl of the Calcium Assay Buffer included in the kit were added to each well, mixed gently, and incubated for 10 minutes in room temperature, protected from light. The plate was read at 575 nm using a microplate reader (Molecular Devices, San Jose, CA) to measure intracellular calcium for 1 X 10^3 cells.

2.3 Results

2.3.1 Klotho ameliorated albuminuria and glomerular injury in db/db mice

After completed 8 weeks of rKL injection, we examined urine albumin and glomerular status for all mice. rKL significantly reduced albuminuria, and increased urinary klotho excretion (Figure 2.1). We speculated that decreased albuminuria by rKL treatment is due to glomerular protection

in db/db mice. To demonstrate the glomerular protective effect, we employed transmission electron microscopy (TEM) to visualize whether podocytes are protected by rKL in db/db mice. Figure. 2.1C clearly shows that glomerular injury markers, such as glomerular basement membrane (GBM) thickening and foot process effacement evident in db/db mice, were significantly ameliorate by rKL treatment. Furthermore, we confirmed that glomerular enlargement presented in db/db mouse kidney is ameliorated by rKL treated by masson trichome staining. Taken together, these results indicate that klotho ameliorated diabetic glomerular injury and decreased albuminuria in db/db mice.

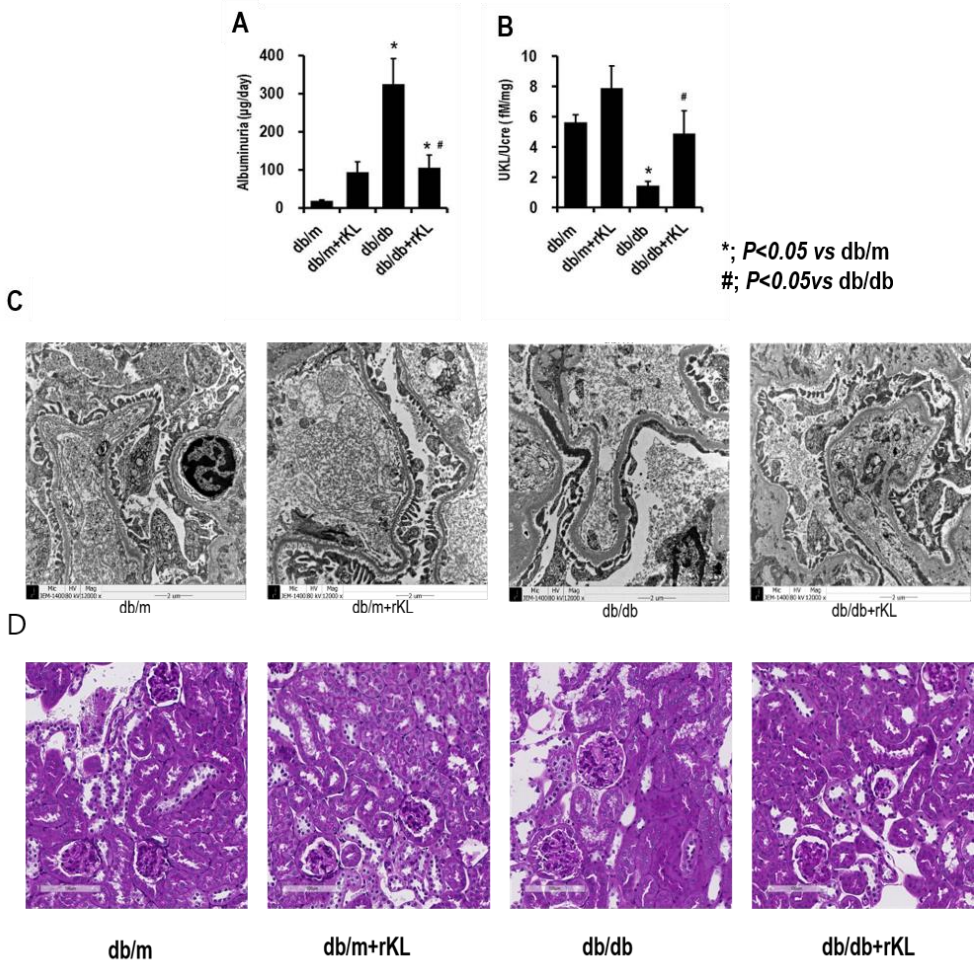

Figure 2.1 Increased α-klotho ameliorated albuminuria, and protected foot process effacement in db/db mice. (A) analysis of albuminuria from all mice. (B) analysis of unine klotho (uKL) from all mice. (C) glomerulus status observed by TEM. Note that diabetic symptoms, such as membrane thickening and foot process effacement, are seen in db/db mice, whether they do not present in db/db+rKL.

2.3.2. Glomerular protection in *db/db* mice by Klotho is through suppression of TRPC6 in podocytes

Then, we hypothesized that glomerular protection by rKL,in a diabetic nephropathy model is mediated by reducing TRPC6 expression in podocytes. Western blot analysis showed that increased TRPC6 expression in db/db mice, was suppressed by rKL treatment (Figure 2.2). Moreover, rKL successfully inhibited not only Pi3K, which is known to induce the exocytosis of TRPC6, but NOX4, as well, which is involved in diabetes-mediated increase in TRPC6. Therefore, rKL mitigated diabetic glomerulopathy by suppressing TRPC6 in podocytes, and rKL-mediated suppression of TRPC6 is through inhibition of both Pi3K and NOX4.

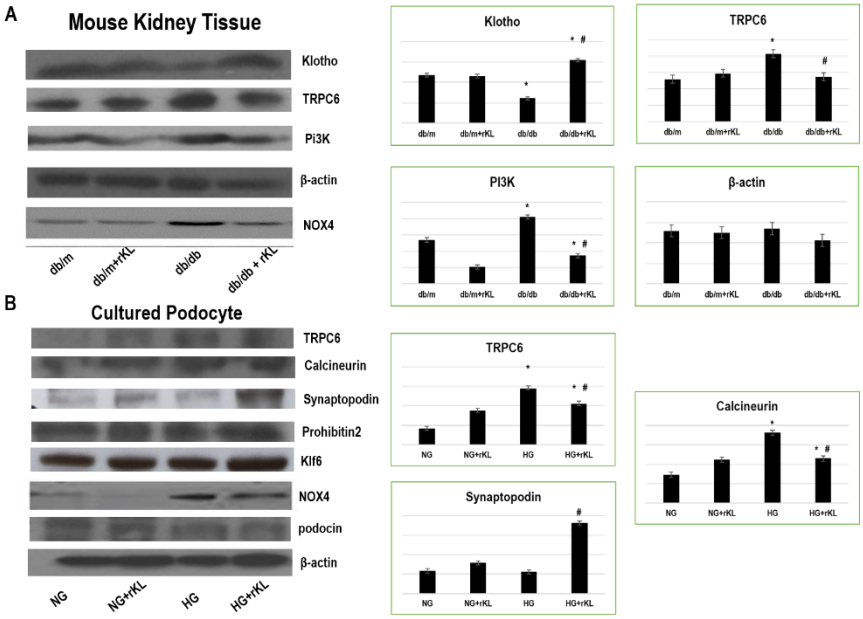

Figure 2.2 rKL treatment reduced TRPC6 and NOX4 expression in db/db mice and HG-treated cultured podocytes. (A) rKL decreased renal TRPC6, Pi3K, and NOX4 expression in db/db mice. (B) rKL reduced TRPC6, calcineurin expression on podocytes, and therefore increased synaptopodin in cultured podocytes.

2.3.3 Klotho suppressed HG- mediated increase of TRPC6 in cultured podocytes

We further checked whether HG-induced TRPC increase is suppressed by rKL by immunofluorescence (IF) assay using podocytes. As expected, red fluorescence representing TRPC6 expression is the highest in HG group, which is significantly decreased by rKL (Figure 2.3). We confirm that klotho protects podocyte from diabetes, therefore reduce albuminuria.

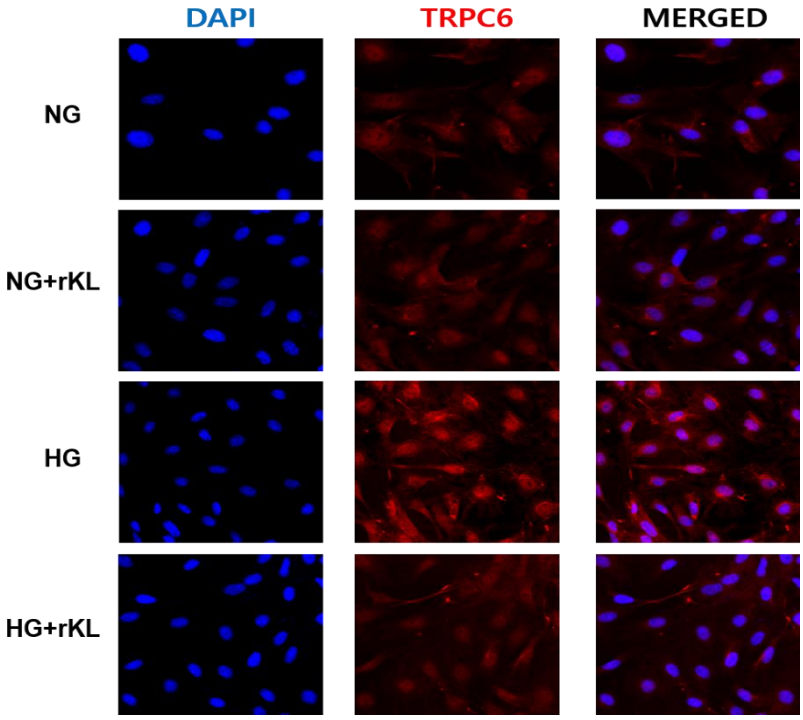

Figure 2.3. rKL suppressed HG-mediated TRPC6 increase in cultured podocytes. Through immunofluorescence (IF) assay, we present TRPC6 (red), is enhanced in high glucose (HG) exposed podocytes, whereas rKL prevented such increase similar to normal glucose (NG) treated podocytes.

2.3.4 In HG condition, klotho resulted in reduced intracellular calcium, recovered synaptopodin, and therefore improved cell survival in cultured podocytes

Since klotho is shown to suppress TRPC6 and to inhibit HG-induced calcineurin expression in the podocytes, we, then, explored whether these changes result in increased synaptopodin expression and improved cell survival of cultured podocytes in HG condition. MTT assay clearly resulted in increased number of alive podocytes by rKL in HG condition. In addition, HG elevated intracellular calcium level from podocytes, and rKL suppressed such increase.

High glucose completely abolished synaptopodin, probably due to increased calcineurin which degrades synaptopodin. However,

synaptopodin expression was recovered after rKL treatment in HG condition. These results indicate that rKL suppresses HG-induced increase in TRPC6 and calcineurin, therefore protects the podocyte integrity in a diabetic condition (Figure 2.4).

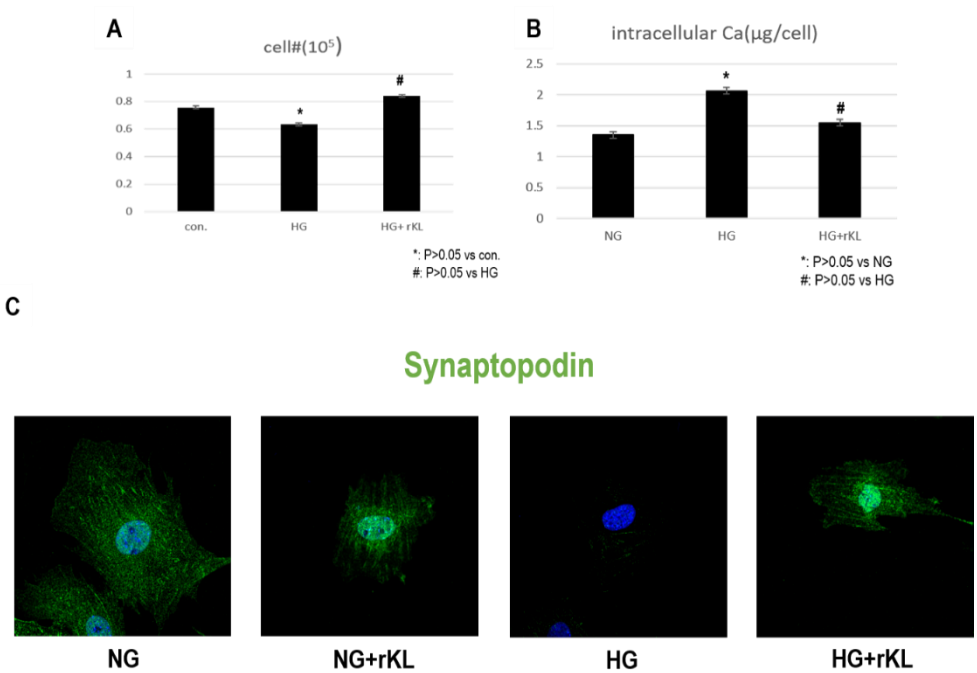

Figure 2.4. rKL improved podocyte survivor, reduced intracellular calcium, and recovered synaptopodin in HG. (A) MTT assay revealed that rKL increased number of live podocytes after HG treatment for 24h. (B) rKL reduced intracellular calcium on podocytes after HG treatment for 24h. C. Synaptopodin expression analysis *in vitro* by IF assay.

2.4 Discussion

Podocyte injury by increased TRPC6 is defined present in many renal diseases, and patients with TRPC6 gain-of-function mutations, such as G109S, showed glomerular sclerosis[23]. TRPC6 is believed to be enhanced either though Pi3K-mediated exocytosis, and/or by ANGII-NOX4-ROS pathway. While Pi3K-mediated exocytosis is known as the main cause of TRPC6 enhancement in CKD model 5/6 nephrectomy mice, ANGII-NOX4-ROS pathway mainly causes TRPC6 increase in diabetic mice[26]. αklotho is reported to protect podocytes by suppressing Pi3K, therefore inhibit TRPC6 in a murine model of CKD[25]. In this study, we showed that αklotho decreases NOX4-ROS in db/db mice, so αklotho inhibits diabetes-induced TRPC6, thereby protect podocytes and glomerulus, and ameliorated albuminuria. Moreover, we found that α-klotho suppressed Pi3K expression in db/db mice, suggesting that α-klotho could be a powerful solution that protects glomerulus from renal dysfunction by suppressing TRPC6 on podocytes.

First, we showed a dramatic increase in urinary calcium excretion and severe glomerular damage in db/db mice were ameliorated by rKL treatment. Then, we presented that the significant increase of TRPC6 expression on both db/db mouse kidney and cultured podocytes were diminished by rKL. In addition, we analyzed podocyte cell survivability, intracellular calcium concentration, and synaptopodin expression and concluded that αklotho protected podocytes by suppressing TRPC6 overexpression, which is normally caused by high glucose condition.

This study identified αklotho as a TRPC6 suppressing factor on podocytes in diabetic situation. We presented that αklotho decreases TRPC6 through preventing both Pi3K-mediated exocytosis, as well as NOX4-Ros mediated enhancement of TRPC6. Therefore, we introduce αklotho as a podocyte protector that inhibits TRPC6 during DN.

Chapter 3. αKlotho ameliorates diabetic nephropathy via LKB1-AMPK-PGC1α-mediated renal mitochondrial protection

3.1 Background

Diabetes is a disease that causes excessive blood glucose, and it is closely related to CKD and aging. Among various the toxins in diabetes, reactive oxygen species (ROS) are thought to be major players[30]. Mitochondrial ROS cause DNA breaks, which activate its repair mechanism. Such DNA repair requires nicotinamide adenine dinucleotide (NAD+), a pivotal cofactor in many metabolic pathways. ROS-mediated DNA damage also inhibits the key glycolytic enzyme glyceraldehyde 3-phosphate dehydrogenase (GAPDH). Depleted NAD+ and GAPDH cause a bottleneck in glycolysis that produces an over-accumulation of upstream glycolytic intermediate molecules, which in turn activates the polyol, protein kinase C, and hexosamine pathways. The activation of those pathways leads to

mitochondrial dysfunction, cellular damage, apoptosis, fibrosis, and inflammation[31,32]. Because mitochondrial dysfunction through ROS accumulation also occurs during aging, it shares a common molecular mechanism with diabetes.

Exercise and calorie restriction are the ultimate cure for diabetes and aging. Active, low-calorie lifestyles cause mitochondrial biogenesis by activating the adenosine monophosphate-activated protein kinase (AMPK) and peroxisome proliferator-activated receptor gamma coactivator 1-alpha (PGC1α) pathway[33,34]. AMPK is a guardian of mitochondrial homeostasis that activates PGC1α, the master regulator of mitochondrial biogenesis[35]. The kidney is a highly metabolic organ with a high mitochondrial density[36]. This high demand for ATP is due to the active reabsorption of sodium, glucose, and other ions from the filtered fluid. This reabsorption occurs mainly in the proximal tubule (PT), which occupies ~90% of the renal cortex and makes up half of kidney mass[37,38]. Therefore, the role of mitochondria is important for renal health. In fact, various renal disorders — acute kidney injury (AKI), renal fibrosis, and DN — are highly related to mitochondrial dysfunction[39].

Those kidney diseases are also associated with a decrease in αKlotho through renal cell damage and the hypermethylation of the *KLOTHO* promotor[40]. Although αKlotho mitigates such disorders, the exact mechanism by which klotho improves renal health is unknown.

In this study, we report that recombinant soluble αklotho (rKL) protein treatment conferred renal mitochondrial protection in diabetic mice by activating the AMPK-PGC1α pathway in the kidney, thereby preventing DN.

3.2. Materials and Methods

3.2.1. Animals

Animal experiments were performed with the approval of the Institutional Animal Care and Use Committee of Seoul National University Hospital (IACUC 15-0055-C1A0). Six-week old male db/db mice (C57BL/6 background) were used in this study. db/m mice were used as the control. All mice were purchased from OrientBio (Seong-Nam, Korea). Baseline

data were collected immediately after their arrival in our lab, and the mice were given 10 days for adaptation. After that, the mice were injected intraperitoneally with either saline, or rKL (R&D SYSTEMS, 1819-KL-050, Ala35-Lys982, 10μg/kg) saline. The injections were given every day for 8 weeks. The mice were housed three or four per cage and kept in a 12h light and 12h dark cycle. 24h urine was collected using a metabolic cage without a food supply a day before sacrifice. Final data were recorded immediately before sacrifice. One kidney from each mouse was fixed in 4% paraformaldehyde and then embedded in paraffin for histologic analysis, and the other kidney was used for western blot analyses.

3.2.2. Cell culture

Mouse S1 proximal and distal tubular cells were generously provided by Dr. Friedman at Pittsburg University. PT cells were incubated in Dulbecco's modified Eagle's medium (DMEM): F12 (Gibco) supplemented with 10% fetal bovine serum (FBS, Gibco) and 1% streptomycin. Mouse distal convoluted tubule cells were incubated in DMEM: F12 in 5% FBS. Cells were starved by culturing them in DMEM: F12 without FBS for 24

hours before they were treated with glucose and rKL. 30mM D-glucose was given for the high glucose (HG) condition, and 5mM D-glucose was given for normal glucose (NG). 10nM of rKL was administered for 24h, along with glucose. All cells were incubated at 37℃ in a humidified atmosphere with 5% CO_2.

3.2.3. Western blotting

Proteins from mouse kidneys and cultured cells were extracted using RIPA lysis buffer. The following primary antibodies were used: klotho (1:2000, KM 2076), PGC1α (1:1000, ab 54481), p-AMPK Thr172 (1:1000, CS 2531), AMPK (1:200, Sc 74461), Rodent OXPHOS mitochondrial complex (1:2000, ab 110413), LKB1 (1:200, Sc 32245), phospho mTOR (1:1000, CS 2971), and TGF-β (1:200, Sc 130448). 40μg of protein from kidney tissue and cultured cells were loaded onto 8% SDS-PAGE gels. Three mice from each group were analyzed.

3.2.4. Transmission Electron Microscopy (TEM)

Pieces of renal cortex tissue were fixed in 4% paraformaldehyde, post fixed in 1% osmium tetroxide, dehydrated in graded alcohols, and embedded in Epon. Ultrathin sections (200–400 Å) were cut on nickel grids, stained with uranyl acetate and lead citrate, and examined at x15,000 using a digital electron microscope (JEM-1400; JEOL Ltd.).

3.2.5. Renal ROS measurement

Cells and sliced renal cortex tissue were incubated in 20μM DCF-DA (ab65319) in PBS at 37℃ for 45 min. After incubation, the samples were washed using PBS. The samples were read at Ex485nm/Em535nm using confocal microscopy (x200, Leica).

3.2.6. Renal NAD+ measurement

Renal NAD+ was measured using a colorimetric kit (Biovision, Milpitas, CA). Briefly, 25 mg of kidney tissue from each mouse was dissected and

homogenized in 500 l of the NAD+/NADH extraction buffer provided. Then, 250 l of homogenate was heated to 60℃ for NADH, and the other half remained unheated to measure NAD+. 25 l of each sample was assayed in a 96-well plate, and the plate was read at 450 nm using a microplate reader (Molecular Devices, San Jose, CA) according to the manufacturer's instructions.

3.2.7. Histologic Analysis

Tubular injury scores were assessed in periodic acid–Schiff (PAS) stained kidney sections. Briefly, kidney injury was assessed by three independent researchers in a blinded manner based on morphologic criteria such as tubular cell necrosis, cast formation, and the loss of tubular brush borders. Overall tubular injury was semi-quantitatively scored by calculating the percentage of affected tubules (0, unaffected; 1, 1%–33%; 2, 33%–66%; 3, 66%–100%) in at least three randomly selected, high-power fields in each section. Apoptotic renal cell nuclei were counted

using TUNEL positive cells. Statistics were calculated by analyzing three random snapshots from each group.

The degree of fibrosis was analyzed by Masson trichrome assay. The blue regions were calculated using ImageJ (NIH, Maryland).

3.2.8. Oxidative phosphorylation (OXPHOS) measurement

After 24h starvation followed by 24h NG or HG exposure, S1 mouse proximal tubule cells and distal convoluted cells were treated with 100 nM TMRE (tetramethylrhodamine ethyl ester perchlorate) and 1 M oligomycin in starvation medium (1% FBS). Cells were incubated at 37 ℃ for 30 minutes, washed in PBS, DAPI treated (1:2000), fixed in 4% paraformaldehyde, and sampled. The samples were examined using confocal microscopy (Leica).

3.2.9. Statistical Analysis

All data are shown as the mean ± SEM. Continuous variables were analyzed using two-tailed t-tests. P values <0.05 were considered statistically significant. All analyses were performed using ImageJ (NIH), Excel (Microsoft), or GraphPad Prism software 7.0 (La Jolla, CA).

3.3 RESULTS

3.3.1. rKL treatment reduced body weight, serum glucose, and albuminuria in db/db mice

Compared with db/m mice, db/db mice had diabetic phenotypes such as obesity, albuminuria, hyperglycemia, and increased renal ROS. Those diabetic phenotypes were significantly ameliorated by rKL injection. In db/db mice, rKL treatment reduced body weight and blood glucose by ~14% (Figure 3.1). Thus, all the major disorders of diabetes were ameliorated by rKL.

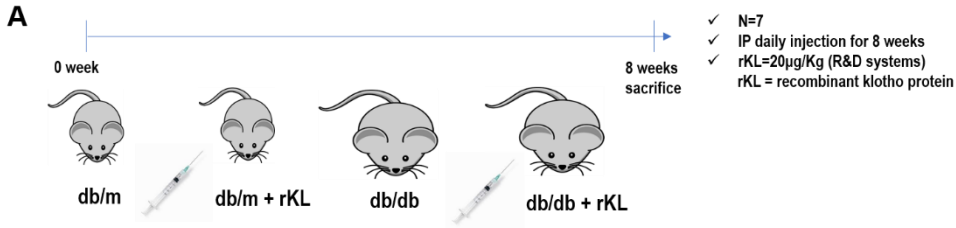

B

Body Weight (g)		
	0 Week	8 Weeks
db/m	21.08±0.52	28.25±0.5
db/m + rKL	22.36±0.31	28.89±0.88
db/db	29.02±0.52	47.64±0.72
db/db + rKL	27.02±0.62	41.70±0.62

Blood Glucose (mg/dl)		
	0 Week	8 Weeks
db/m	115.14 ± 3.74	112.83 ± 4.04
db/m + rKL	112.43 ± 3.22	115.17 ± 2.93
db/db	322.86 ± 12.29	314.33 ± 20.97
db/db + rKL	344.57 ± 11.96	271.17 ± 15.76

C

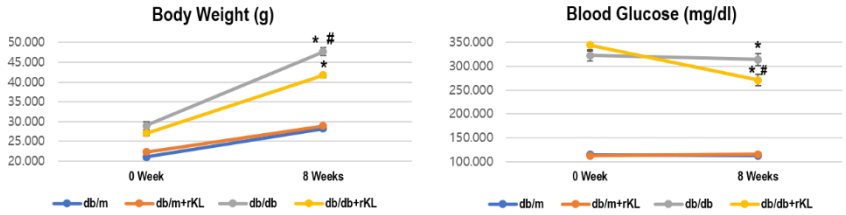

Figure 3.1. Diabetic phenotypes improved by rKL treatment. (A) db/m and db/db mice were injected intraperitoneally either with rKL or vehicle (PBS) for 8 weeks. (B) Body weight and blood glucose at baseline and week 8; rKL treatment reduced both of them significantly in db/db mice, but did not bring the levels close to those of the control groups. (C) Visualized graphs for (B). *: $P < 0.05$ vs db/m. #: $P < 0.05$ vs db/db.

3.3.2. Diabetes-induced proximal tubular damage and renal ROS were mitigated by rKL treatment

In db/db mice representing T2D, damage and apoptosis of tubular cells produced renal fibrosis. rKL treatment of the db/db mice reduced tubular injury and the number of apoptotic tubular cells, as shown by PAS staining and the TUNEL assay. rKL-treated db/db mice also showed significantly diminished renal fibrosis compared with the db/db control. Moreover, ROS staining using DCF-DA identified a significantly reduced intensity in the PT of rKL-treated db/db and S1 mouse PT cells (Figure 3.2). These results indicate that tubular damage in T2D kidneys was ameliorated by rKL.

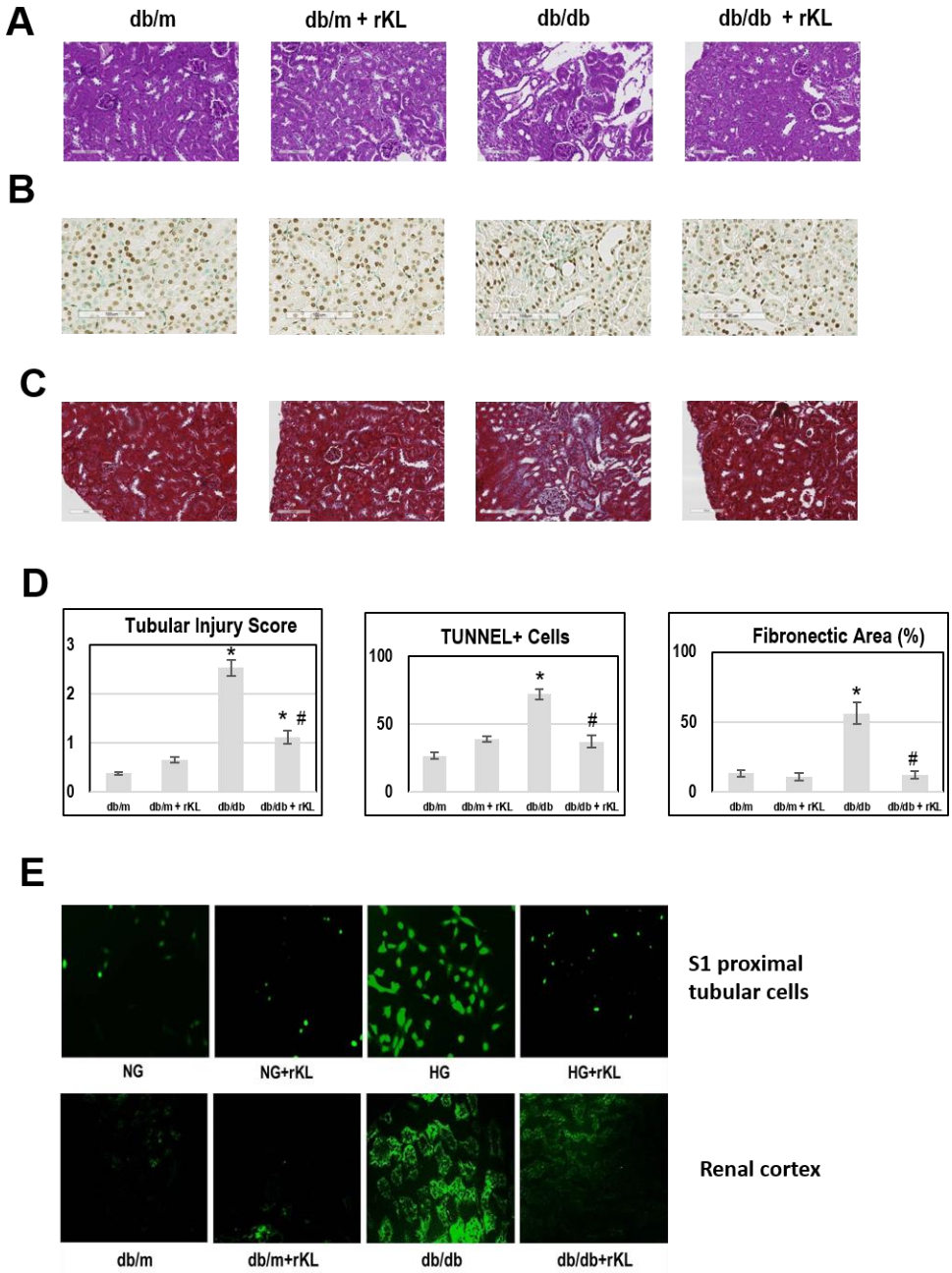

Figure 3.2. rKL produced renoprotective effects in db/db mice. (A) Renal tubular injury analyzed using periodic acid-Schiff staining. (B) Apoptotic cells analyzed by the TUNEL assay. (C) Fibrotic area (in blue) from trichrome staining.

(D) Visualized graphs of (A), (B), and (C). *: $P < 0.05$ vs db/m. #: $P < 0.05$ vs db/db. (E) Reactive oxygen species (ROS) from mouse kidneys and S1 mouse proximal tubular cells, measured using DCF-DA staining.

3.3.3. rKL increased renal AMPK-PGC1α expression and recovered mitochondria in db/db mice

We reasoned that the renoprotective effects of rKL occurred through the activation of the AMPK-PGC1α pathway, which conferred renal mitochondrial protection. Western blot analyses of mouse kidneys revealed that rKL significantly increased phospho-AMPK and PGC1α levels in db/db mice. Moreover, rKL decreased renal mTOR expression, which is a nutrient abundance marker that increases in T2D (Figure 3.3A). Indeed, rKL altered the expression of energy sensing molecules in diabetic mice from nutrient abundant to nutrient depletion-like conditions, thereby inducing mitochondrial biogenesis.

Next, we investigated whether mitochondrial recovery was present in those mice. To observe that, we sliced the kidney cortexes and examined them though TEM. We observed plenty of damaged

mitochondria throughout the renal cortexes of the db/db control mice (Fig. 3.3B, marked by arrows), whereas very few were visible in the renal cortexes of rKL-treated db/db mice. These results indicate that rKL successfully increased AMPK-PGC1α and thereby induced mitochondrial protection in diabetic kidneys.

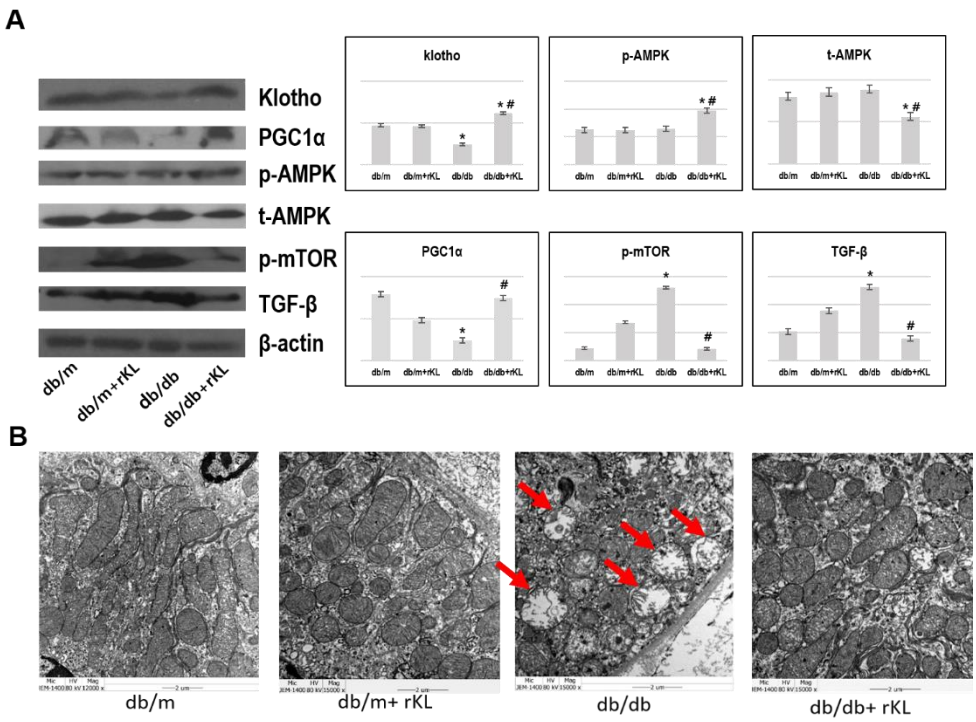

Figure 3. rKL increased p-AMPK and PGC1α, thereby producing intrarenal mitochondrial protection in db/db mice. (A) rKL increased p-AMPK and PGC1α and decreased p-mTOR and TGF-β in db/db mice, as shown by western blot. *: $P < 0.05$ vs db/m. #: $P < 0.05$ vs db/db. (B) TEM images of proximal tubule cell mitochondria. Damaged mitochondria are marked with arrows.

3.3.4. rKL restored HG-induced mitochondrial damage and increased OXPHOS in cultured proximal tubular cells

To determine whether klotho directly protects mitochondria, apart from its glucose-lowering effects, we performed an *in vitro* study using S1 PT cells. A Mitotracker Red analysis revealed that more functional mitochondria were present in HG + rKL treated cells than in cells treated with HG alone (Figure 3.4A). Along with the decreased ROS shown in Figure 2, this indicates that rKL directly protects mitochondria in renal tubular cells exposed to 30 mM glucose.

Previous studies showed that diabetic kidneys had decreased mitochondrial OXPHOS at the subunit level, especially complexes 1, 3, and 4[41]. After confirming mitochondrial recovery, we hypothesized that rKL improves OXPHOS in diabetic kidneys by increasing the electron transport of the subunit complexes. In our animal experiments, the western blots showed that rKL significantly increased mitochondrial complexes 1, 2, 3, and 4 in db/db mice (Figure 3.4B).

We then designed a mitochondrial membrane potential measurement to verify that rKL increased OXPHOS in the HG condition. We measured the mitochondrial membrane potential from mouse S1 PT cells by administering TMRE, a reversible membrane-potential sensitive dye, in four conditions (NG, NG + rKL, HG, and HG + rKL). TMRE red fluorescence was weak in all four conditions (Figure 3.4C), indicating either functional mitochondria with a proton gradient neutralized by ATP synthase or nonfunctional mitochondria with inhibited membrane potential. Therefore, we applied TMRE plus oligomycin, which blocks ATP synthase. In those results, all conditions except HG exhibited TMRE fluorescence, with HG + rKL having the strongest mitochondrial potential (Figure 3.4D). Therefore, we conclude that rKL treatment restored mitochondrial numbers as well as OXPHOS function in diabetic mice.

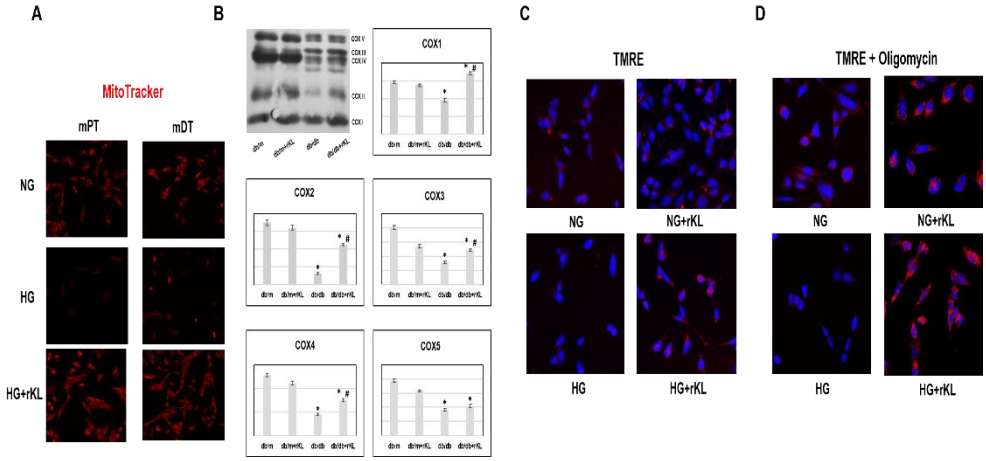

Figure 3.4. rKL improved mitochondrial function. (A). Mitotracker Red on mouse proximal tubular cells (mPT) and mouse distal tubular cells (mDT). (B) rKL increased renal mitochondrial electron transport complexes 1, 2, 3, and 4 in db/db mice. *: $P < 0.05$ vs db/m. #: $P < 0.05$ vs db/db. (C) Mitochondrial membrane potential analysis by TMRE staining. No significant difference between groups was observed. (D) When ATP synthase was inhibited by oligomycin, all groups except HG showed strong membrane potential, with HG + rKL being the strongest. Original magnification x80.

3.3.5. rKL dramatically reversed renal NAD+ shortage in diabetic mice by inducing *de novo* synthesis of NAD+

NAD+ is a cofactor for many enzymes involved in energy metabolism, including the AMPK-PGC1α pathway, which transfers high energy electrons to mitochondria[34]. Declining NAD+ is a hallmark of aging,

and as well as mitochondrial dysfunction[42]. Recently, NAD+ has emerged as a powerful renoprotective factor. Increased renal NAD+ is reported to confer protection in various renal diseases in both animal experiments and humans[43]. We hypothesized that rKL would increase renal NAD+ in diabetic mice, thereby ameliorating diabetic kidney disease. As expected, rKL-treated diabetic kidneys exhibited a dramatic increase in renal NAD+ compared with the diabetic control (Figure 3.5A). We also discovered that rKL decreased α-amino-β-carboxymuconate-ε-semialdehyde decarboxylase (ACMSD) in db/db mice. Because ACMSD inhibits *de novo* synthesis of NAD+, its decrease by rKL indicates that rKL enhanced renal NAD+ in db/db mice through *de novo* synthesis (Figure 3.5B).

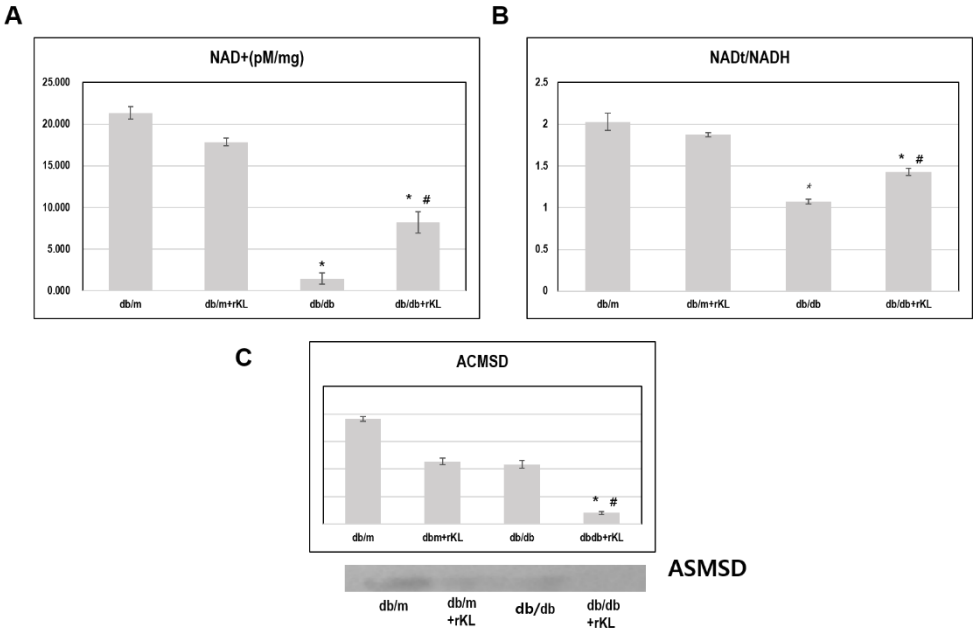

Figure 3.5. rKL produced a dramatic increase in renal NAD+ in db/db mice by inducing *de novo* synthesis. (A) Renal NAD+ per mg of tissue analyzed by colorimetric kit. (B) Calculating total NADt (NAD+ and NADH) divided by NADH revealed an increase in NAD+ in the db/db + rKL condition. (C) Renal α-amino-β- carboxymuconate-ε-semialdehyde decarboxylase (ACMSD), which inhibits NAD+ *de novo* synthesis, decreased in the db/db +rKL group. *: $P < 0.05$ vs db/m. #: $P < 0.05$ vs db/db.

3.3.6. rKL recovered HG-induced mitochondrial damage in proximal tubular cells without FGF23

αklotho is most well-known as a co-receptor for FGF23 signaling through an interaction with FGFR1. However, klotho has effects beyond

FGF23 signaling, and klotho-induced mitochondrial recovery does not seem to be related to FGF23 signaling (which is SGK-ERK). By administering AZD4547, a novel FGFR1 inhibitor[44], to S1 proximal tubular cells, we sought to determine whether klotho-induced activation of AMPK-PGC1α is FGF23-independent. In that experiment, klotho successfully activated AMPK-PGC1α and increased the number and OXPHOS of mitochondria independently of FGF23-FGFR1 activation (Fig. 3.6A).

3.3.7. Among various upstream molecules of AMPK, rKL activates LKB1

Given the FGF23-independent activation of AMPK-PGC1α, we decided to find which upstream molecules of AMPK klotho activates. In addition to exercise and fasting, liver kinase beta 1 (LKB1) and calcium-sensitive kinase CAMMK2 are major upstream molecules that activate AMPK[45]. Our western blot analyses of mouse kidneys and S1 proximal tubular cells indicate that LKB1 (but not CAMMK2) is increased by rKL

(Fig. 3.6B), indicating that klotho activates AMPK through LKB1. Moreover, rKL significantly increased mitofusin 1 (MFN1), a marker of mitochondrial fusion whose expression decreases during DN[46]. Klotho also increased renal sequestosome 1 (SQSTM1, also known as P62), which is a marker for autophagy[47], in db/db mice, further supporting that mitochondrial protection occurs. Therefore, we report that αklotho enhances the AMPK-PGC1α pathway through LKB1, which results in increased mitofusion and autophagy in diabetic kidneys.

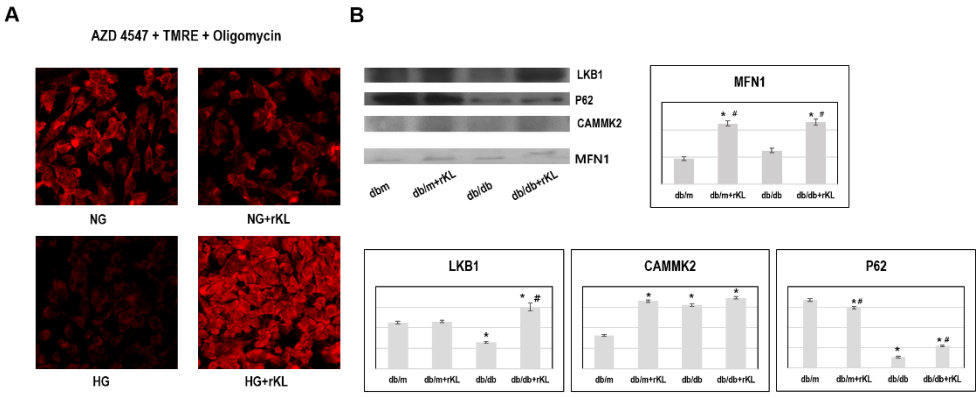

Figure 3.6. Klotho activates the AMPK-PGC1α pathway through LKB1, not FGF23. (A) Klotho increases OXPHOS in HG-exposed mouse proximal tubule cells when FGFR1 is inhibited by AZD 4547. (B) Among the upstream molecules that activate AMPK, klotho increased LKB1, but not CAMMK2. Klotho also increased mitofusin 1 (MFN1) and sequestosome 1 (P62) in db/db mice, indicating increased mitofusion and autophagy, respectively. *: $P < 0.05$ vs db/m. #: $P < 0.05$ vs db/db.

3.4. DISCUSSION

Both diabetes and aging involve mitochondrial dysfunction. Many agents intended to confer mitochondrial protection are effective against both diabetes — including DN — and aging[48].

In this study, we found that tubular injury occurs in T2D-induced DN and that the anti-aging molecule αKlotho protects renal mitochondria by activating the LKB1-AMPK-PGC1α pathway. αKlotho also increased NAD+ and OXPHOS and decreased DN-related factors such as obesity, serum glucose, and renal ROS, thereby ameliorating DN (Fig. 3.7). Kidney tissue possesses a high density of mitochondria and demands a large amount of ATP to preserve homeostasis[36], indicating that mitochondrial health is important in maintaining renal health. Many studies have shown that AMPK protects against various types of renal dysfunction[49], and its level declines with aging[50]. We strengthened the connection between diabetes and aging, and we further discovered additional anti-aging (and anti-diabetes) roles of klotho.

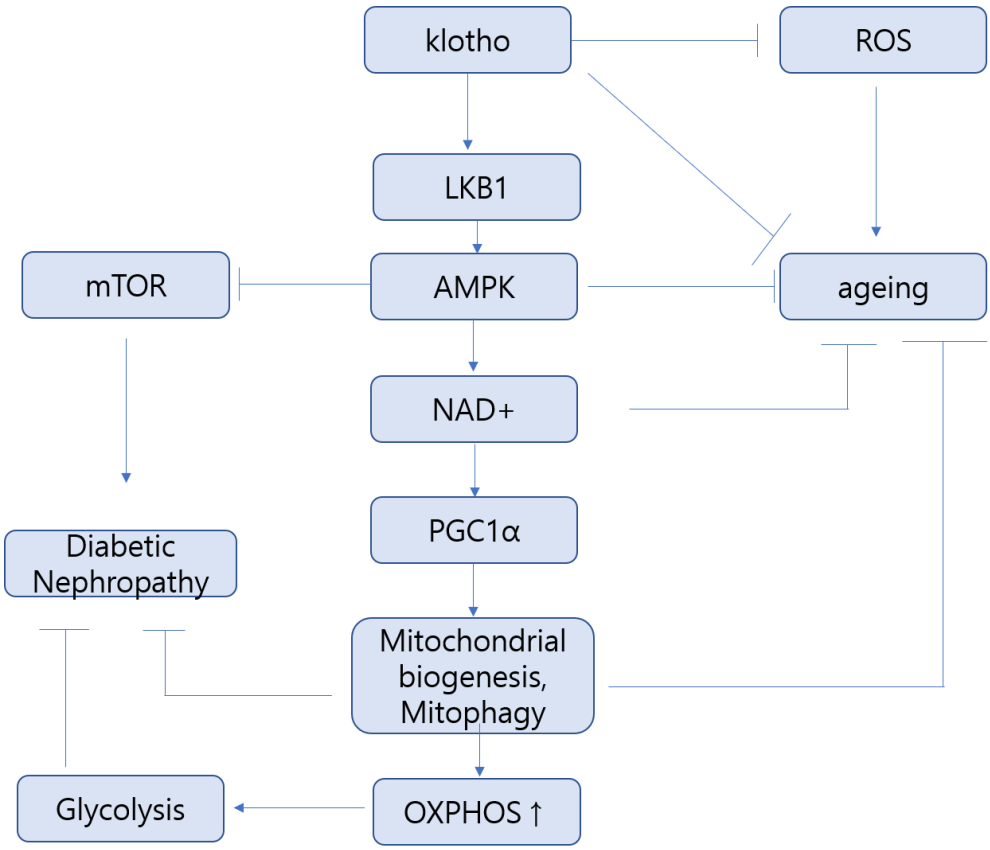

Figure 3.7. αklotho activates the AMPK-NAD+-PGC1α pathway by increasing LKB1, thereby exhibiting mitochondrial protection in diabetic kidneys.

Another important finding of this study is a dramatic increase in renal NAD+ in db/db mice treated with αklotho. NAD+ has at least two important cellular functions: 1) to transport high-energy electrons to

mitochondria, and 2) as a substrate for sirtuins, which are related to life elongation[42]. NAD+ has recently emerged as a powerful renoprotective molecule. Oral treatment with nicotinamide, a precursor molecule of NAD+, is reported to improve renal function in AKI patients. Moreover, an animal study indicated that inducing *de novo* NAD+ synthesis by administering an ACMSD inhibitor improved AKI and fatty liver disease through increased sirtuin and mitochondrial function[51]. NAD+ is also reported to stabilize telomerase[52], further suggesting klotho's anti-aging role in mediating gene stability. Our study has shown that klotho not only enhanced renal NAD+ but also abolished ROS, indicating that klotho could widen the bottleneck in glycolysis. The liver and kidney are the organs with the highest exposure to toxic molecules, and thus they require a sufficient amount of NAD+ for detoxification. They are also the two major organs expressing the klotho protein, αklotho in the kidney and βklotho in the liver. Further study is required to define the relationship between klotho and NAD+ and how it affects aging, energy metabolism, and telomere protection.

Although glomerular damage is the main disorder in DN, PT injuries are also important factors to consider. A recent mouse study reported that suppressed autophagy in the PT is related to renal injury in db/db mice, and rapamycin ameliorated DN in those mice[53]. Therefore, treating tubular injuries is important when treating DN. Given that, we suspected that apoptosis-mediated PT injury could occur in db/db mouse kidneys. Furthermore, because klotho induces a renoprotective effect by inducing autophagy[54], we expected rKL treatment to recover the PT in db/db mice. Whereas T1D causes enhanced autophagy in the PT, PT autophagy is decreased in T2D mouse models, even during fasting[53]. Given that αklotho induces autophagy in db/db mice, which even starvation failed to increase, we suggest that klotho could have tremendous renoprotective effects.

The present study in db/db mice showed that LKB1 is the main upstream molecule of AMPK that is activated by rKL. LKB1 directly activates AMPK by phosphorylating Thr172 in the α subunit of AMPK, which is critical for its activation[45]. Distal tubule–specific deletion of *Lkb1* resulted in progressive CKD in mice, with significantly lowered AMPK and

PGC1α[55]. If the *Lkb1* KO mice had intact klotho expression, αklotho must have activated AMPK though LKB1 rather than interacting directly with AMPK. Given that LKB1 is a well-known tumor suppressor, this connection might explain the anti-cancer effects of klotho.

This study has several limitations. First, rKL significantly decreased serum glucose in db/db mice, which could mediate the mitochondrial protection. We therefore performed an *in vitro* study using mouse S1 PT cells at the same glucose concentration and observed significant mitochondrial recovery with klotho treatment. Our results thus warrant future study on the mechanistic pathway of renal mitochondria protection by klotho. In addition, we used only T2D mice, so how rKL would affect T1D remains to be discovered. PT autophagy is enhanced in T1D kidneys, whereas it is suppressed in T2D, which is highly related to tubular injury in db/db mice. Therefore, rKL might have different effects on streptozotocin-treated mice. Moreover, our results cannot explain the mechanism of weight loss in db/db mice. One possible explanation is that klotho treatment elicits the βKlotho effect, which causes decreased obesity in mice. A previous study reported that delivering the *klotho* gene in an

AKI mouse model using adeno-associated virus increased not only renal, but also hepatic klotho (βKlotho) gene expression[56]. Moreover, a recent randomized trial reported that exercise increases plasma-soluble klotho in middle-aged adults[57]. Future studies are warranted to investigate how rKL affects serum FGF19 and 21, liver βklotho expression, and brown adipose function. For example, it is worth learning whether UCP1 expression would be increased by rKL and induce body thermogenesis.

This study discovered a new renoprotective role of the antiaging molecule klotho. In db/db mice, klotho protected mitochondria by activating the AMPK-PGC1α pathway, increasing NAD+ and OXPHOS and reducing ROS and mTOR in the kidney, thereby mitigating DN. These results indicate that klotho could play a renoprotective role by targeting mitochondrial dysfunction, similar to antioxidants and OXPHOS enhancers. Our results suggest that αklotho could be used to treat DN and have highly renoprotective effects beyond those of exercise and calorie restriction.

Chapter 4. Soluble αklotho anchors TRPV5 to the distal tubular cell membrane independent of FGFR1 by binding TRPV5 and galectin-1 simultaneously

4.1 Background

Diabetic nephropathy (DN) is the leading cause of end-stage renal disease (ESRD)[1]. Hypercalciuria is one of the renal manifestations of DN, caused by failure to absorb filtered calcium in the renal tubule[58]. Such Ca^{2+} loss in DN is associated with bone fracture, osteopenia, and nephrocalcinosis[59]. Therefore, knowing the mechanism and control of hypercalciuria is important. Transient receptor potential vanilloid type 5 (TRPV5) is a glycoprotein responsible for managing renal calcium reabsorption in the distal tubule, and its expression declines in DN,

resulting in hypercalciuria[60]. Therefore, to increase TRPV5 expression would positively impact the treatment of hypercalciuria.

αklotho is a type 1 transmembrane antiaging protein mainly expressed in the renal distal tubule, and one of its functions is to increase TRPV5 through fibroblast growth factor 23 (FGF23) signaling[5,61]. αKlotho has a short intracellular domain (~35 amino acids) and a long extracellular domain (~950 amino acids) that contains two repeats with 21% amino acid identity, namely the KL1 (~450 amino acids) and KL2 (~430 amino acids) domains[62]. The full length α-Klotho protein (~140 kD) can be cleaved by membrane secretases which release the extracellular domain (~130 kD) into circulation[63,64]. This soluble αklotho (sKL) can circulate in the blood, urine, and cerebrospinal fluid, with effects beyond FGF23[7,65].

The mechanism by which soluble αklotho increases TRPV5 was originally thought to occur through removal of terminal sialic acids from α2-3-sialyllactose in TRPV5. This process was thought to expose disaccharide galactose-*N*-acetylglucosamine (GalNAc) on TRPV5, which is

the binding site for galectin-1[66]. Galectin-1 is an abundant lectin in the extracellular matrix, which binds and therefore holds certain receptors and ion transporters to the cell surface, thereby inhibiting their endocytosis. Galectin-1 holds cytokine receptors and glucose transporters, thus increasing their abundance at the cell surface[67,68]. It was believed that αklotho creates a binding site for galectin-1 to TRPV5 by cleaving terminal sialic acids[66]. However, a structure study of α2-3-sialyllactose revealed that soluble αklotho binds to, rather than alters glycosylation of, α2-3-sialyllactose[69]. Therefore, soluble αklotho does increase TRPV5 by mediating interaction with galectin 1, but the exact mechanism that was once believed solved is again elusive.

Given that αklotho levels decline during renal disease via gene methylation[70], that α-klotho binds to TRPV5 via α2-3-sialyllactose, and that αklotho manages TRPV5 to interact with galectin-1, we hypothesized that soluble α-klotho itself interacts with both TRPV5 and galectin-1, therefore tethering TRPV5 on the apical membrane of distal tubular cells in a galectin-1-dependent manner.

4.2 Materials and methods

4.2.1. Animals

C57BL/6J male mice aged 7 weeks were purchased from Envigo RMs Limited (Envigo Ltd, UK). A puromycin aminonucleoside (PAN) mouse model was induced by intraperitoneal (i.p) injection of PAN (100 mg/kg, Sigma, MO, USA) in phosphate buffered saline (PBS) every two weeks (n=7).

Six-week old male db/db mice (C57BL/6 background) were used as the study group, while db/m mice were used as the control group. All mice were purchased from OrientBio (Seong-Nam, Korea). Baseline data were collected immediately after arrival, and mice were given 10 days for adaptation. After that, mice were injected intraperitoneally with either normal saline (KisanBio, Korea) or recombinant αklotho (rKL, R&D SYSTEMS, 1819-KL-050, Ala35-Lys982, 10μg/kg) in normal saline. The dose of the recombinant Klotho was decided as previous reported elsewhere[71]. The injection was done every day for 8 weeks. Three or four mice were housed per cage and remained in a 12h light and 12h

dark cycle. Urine for 24h was collected at the eighth week using a metabolic cage without food supply. Final data were recorded immediately before sacrifice. One kidney from each mouse was fixed in 4% paraformaldehyde and then embedded in paraffin for histologic analysis, and the other kidney was used for western blot analysis. Animal experiments were performed with the approval of the Institutional Animal Care and Use Committee of Seoul National University Hospital (IACUC 13-0392, 15-0055, 15-0055-C1A0).

4.2.2. Cell culture

Mouse distal tubular cells were generously obtained from Dr. Friedman at the University of Pittsburgh, and cell culture was carried out as previously described[72]. Cells were incubated in Dulbecco's modified Eagle's medium (DMEM): F12 (Gibco) supplemented in 5% fetal bovine serum (FBS, Gibco) and 1% streptomycin. Cells were starved by culture in DMEM: F12 without FBS for 24 hours before being treated with glucose and rKL. For the high glucose (HG) condition, 30 mM D-glucose was

given, while 5 mM D-glucose represented normal glucose (NG) levels. Cells were treated with 10nM of rKL, along with glucose for 24 h. All cells were incubated at 37℃ in a humidified atmosphere of 5% CO_2. Treatment with 1 uM of AZD4547 and 200 uM of OTX008 followed.

4.2.3. Western Blotting

Protein from mice kidney and cultured cells was extracted using LIPA lysis buffer. Primary antibodies were used as follows: α-klotho (1:2000, KM 2076), TRPV5 (1:200, SC 30186), galectin-1 (1:200, SC 166618), FGFR1 (1:1000, ab58516), p-ERK (CS 4370S), ERK (CS 4695S), p-SGK, SGK (SC-15885), and WNK4 (1:SC-20475). Protein from kidney tissue and cultured cells, 40 μg, was loaded into 8% SDS-PAGE gel. Three mice from each group were analyzed.

4.2.4. Immunohistochemistry (IHC)

After fixation in 10% formalin neutral buffered solution immediately after sacrifice, kidneys and lung were embedded in paraffin. IHC was performed using an Ultra-sensitive ABC Rabbit IgG staining kit and following the manufacturer's specifications (Thermo Scientific, Rockford, IL, USA). Samples were rehydrated in decreasing ethanol solutions, then immersed phosphate buffered saline for 10 min followed by quenching in 3% hydrogen peroxide. Slides were blocked for 30 minutes in the kit's blocking solution. α-klotho antibody (Santa cruz biotechnology, CA, USA), FGFR1 antibody (Abcam, Cambridge, MA, UK), and TRPV5 antibody (Santa cruz biotechnology, CA, USA) were applied to slides and incubated for an hour. Secondary horseradish peroxidase (HRP)-conjugated antibodies were applied following another PBS wash and incubated for 1 hour as indicated. Slides were rewashed for 10 min with PBS, and then the ABC reagent was applied for 30 minutes. Immunostaining was detected using a Metal Enhanced DAB Substrate Kit (Thermo Scientific, Rockford, IL, USA).

4.2.5. Immunofluorescence

Primary antibodies were used as follows: αklotho (SC-22218, 1:50), TRPV5 (SC-30186, 1:50), and galectin-1 (SC-166618, 1:50).

Secondary antibodies were used as follows: Donkey Anti-Goat IgG Alexa Fluor 488 (ab150129, 1:2000), Goat Anti-Mouse IgG Alexa Fluor 555 (ab150114, 1:2000), and Donkey Anti-Rabbit IgG Alexa Fluor 647 (ab150075, 1:2000). Cells were treated with DAPI (Carl Roth, 6843.1, 1:2000) to stain the nucleus.

4.3 RESULTS

4.3.1. Biological and physiological analysis

Biological and physiological data are shown in Table 1. A puromycin aminonucleoside (PAN) model was used for proteinuric control. The PAN mouse model was established by injecting 150 mg/kg PAN intraperitoneally (ip) every 2 weeks. There was no significant difference among the control, PAN, and db/m mice in body weight (wt) or blood

pressure (BP), but these parameters were elevated in the db/db mice (Table 4.1). Renal function was evaluated through serum creatinine (Cre) and blood urea nitrogen (BUN) levels, with serum creatinine showing a significant increase in db/db mice compared to other groups.

			Serum						Urine	
	Body wt (g)	Kidney wt (mg)	Glucose (mg/dl)	B.P (mmHg)	Cr (mg/dl)	BUN (mg/dl)	Ca (mg/dl)	P (mg/dl)	Ca/Cr	P/Cr
Sham	28.36 ±0.57	67 ± 8	118 ± 4	116 ± 3	0.33 ±0.02	27.1 ±1.0	10.9 ±0.3	7.6 ±0.2	0.28 ±0.07	2.91 ±0.31
PAN	27.97 ±0.5	74 ± 7	119 ± 3	113 ± 2	0.30 ±0.01	30.2 ±0.7	8.9 ±0.2	8.1 ±0.3	0.29 ±0.09	3.12 ±0.29
db/m	28.25 ±0.5	70 ± 10	117 ± 2	117 ± 1	0.56 ±0.02	27.7 ±1.4	8.6 ±0.1	6.4 ±0.3	0.38 ±0.05	3.26 ±0.24
db/m+rKL	28.89 ±0.88	77 ± 11	115 ± 3	117 ± 3	0.37 ±0.10	22.8 ±2.0	8.7 ±0.2	8.5 ±0.8	0.25 ±0.04	2.31 ±0.44
db/db	47.64 ±0.72 *#$	195 ± 18	314 ± 21 *#$	135 ± 4 *#$	1.02 ±0.01 *#$	27.3 ±1.4	9.8 ±0.1	8.1 ±0.7	0.55 ±0.05 *#$	9.00 ±0.93 *#$
db/db+rKL	41.70 ±0.62 *#$@	178 ± 12	271 ± 16 *#$@	133 ± 2 *#$	0.94 ±0.07 *#$	25.2 ±0.7	9.3 ±0.2	10.5 ±0.9	0.31 ±0.06 @	6.27 ±0.93 *#$@

Table 4.1. General results from mice after 8weeks of rKL treatment.

*: $p < 0.05$ *vs* Sham; #: $p < 0.05$ *vs* PAN; $: $p < 0.05$ *vs* db/m; @: $p < 0.05$ *vs db/db*

4.3.2. Decreased renal αklotho in db/db mice was associated with urinary calcium excretion through TRPV5 downregulation

Next, we examined the albuminuria, αklotho, and Ca^{2+} excretion levels in the urine. As shown in Table 4.1, db/db mice exhibited increased albuminuria and urinary Ca^{2+} excretion levels compared to the db/m mice ($P>0.05$). However, unlike the db/db mice, PAN-injected mice, as the proteinuric control (Figure 4.1A), did not exhibit hypercalciuria (Figure 4.1B). This might be associated with the decreased αklotho levels (UKL/Ucre) evident only in the db/db mice compared to the other three groups (Figure 4.1C). Both PAN and db/db mice showed albuminuria, while only the db/db mice exhibited hypercalciuria and decreased urinary αklotho levels (Figures 4.1). Therefore, we speculated that hypercalciuria is a specific manifestation of DN.

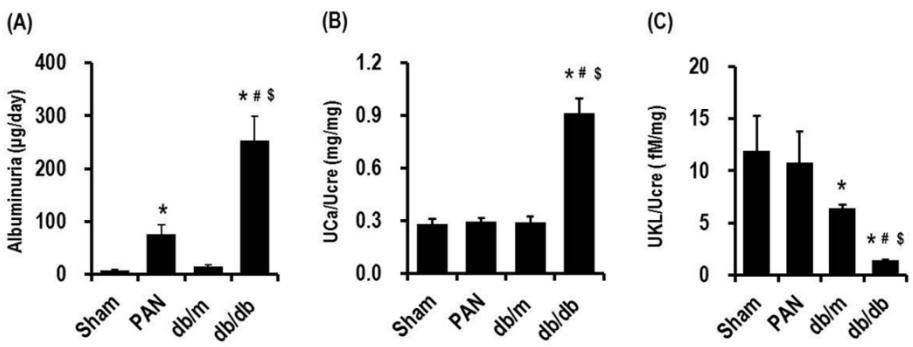

Figure 4.1. Among proteinuric mouse models, only db/db mice showed decreased urinary α-klotho and hypercalciuria. (A) Albuminuria, (B) urinary

calcium excretion, and (C) urine α-klotho (UKL) of sham, PAN, db/m, and db/db mice.

To further investigate the mechanism of Ca^{2+} excretion in db/db mice, we examined mRNA and protein expression of αklotho via RT-PCR (Figure 4.2A) and western blot analysis (Figure 4.2B), along with the TRPV5 expression level in the kidney. The results revealed that mRNA and protein expression levels of αklotho, FGFR1, and TRPV5 were decreased in the db/db mice, but they remained unchanged in the other three groups. Immunohistochemistry (IHC, Figure 4.2C) and immunofluorescence (IF, Figure 4.2D) analysis also showed that αklotho, FGFR1, and TRPV5 were reduced in db/db mice but not in PAN-injected mice. These results suggested that decreased renal αklotho levels in a diabetic kidney caused urinary Ca^{2+} excretion through TRPV5 downregulation.

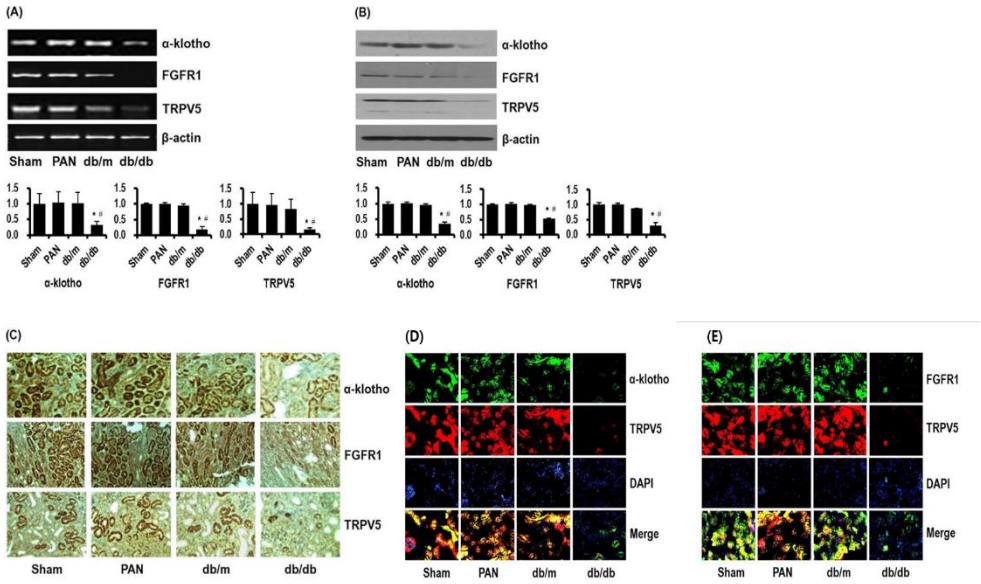

Figure 4.2. Only db/db mice and not PAN mice showed decreased expression of renal α-klotho, TRPV5, and FGFR1. (A) PCR analysis and (B) protein expression compared by western blot. (C) Protein expression analyzed by immunohistochemistry. (D) Tissue protein expression compared through immunofluorescence using a mouse kidney (magnification X 200).

4.3.3. db/db mice treated with rKL prevented urinary Ca^{2+} loss

Next, we confirmed the effects of mouse recombinant αklotho treatment on the murine model of DN. As expected, recombinant soluble αklotho (rKL) improved the albuminuria in db/db mice (Table 4.1). Urinary Ca^{2+} excretion represented by UCa/Ucre was significantly higher in db/db mice, which had been subject to rKL treatment (Figure 4.3A). Urinary αklotho (UKL) levels were decreased in db/db mice, while those treated with recombinant αklotho exhibited upregulated urinary αklotho levels (Figure 3B). This indicates that α-klotho treatment resolves hypercalciuria in db/db mice.

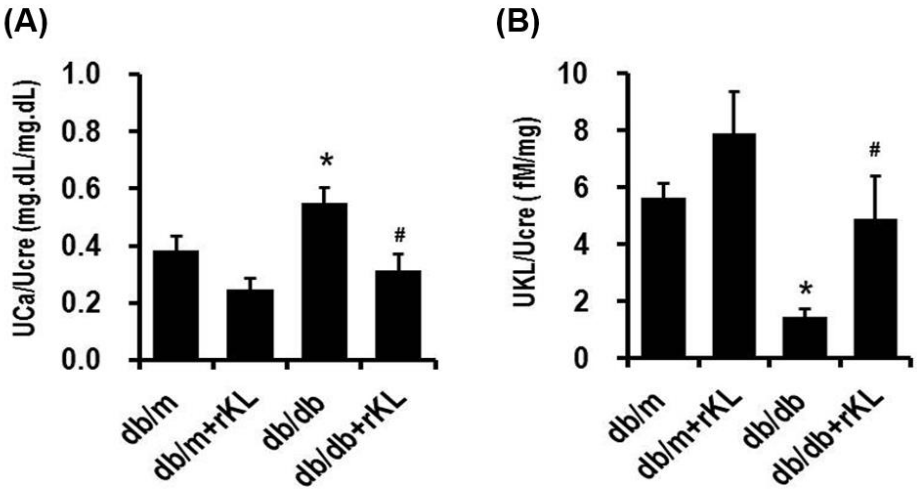

Figure 4.3. rKL significantly improved calciuria in db/db mice. (A) Hypercalciuria mitigated by rKL in db/db mice. (B) Urinary klotho excretion in mice.

4.3.4. Mouse rKL upregulated TRPV5 and α-klotho expression levels in db/db mice

To determine whether diminished Ca excretion by rKL is due to increased TRPV5, we investigated the mRNA and protein levels of αklotho, FGFR1, and TRPV5 in the kidney tissue. The expression of these molecules was significantly decreased in db/db mice, while these molecules were upregulated in the rKL treatment group (Figure 4.4). For further confirmation from the localization of αklotho, FGFR1, and TRPV5 in the

kidney tissue, we performed the IHC and IF analyses. We used lung from wild-type C57BL/6 mice as negative control. As expected, αklotho and TRPV5 were downregulated in db/db mice compared to in non-diabetic groups (i.e., db/m and db/m + rKL groups), but their expression recovered following rKL treatment in the db/db + rKL group (Figure 4.4C and D). Taken together, rKL supplement prevented the downregulation of αklotho, FGFR1, and TRPV5 under diabetic conditions, which in turn ameliorated hypercalciuria.

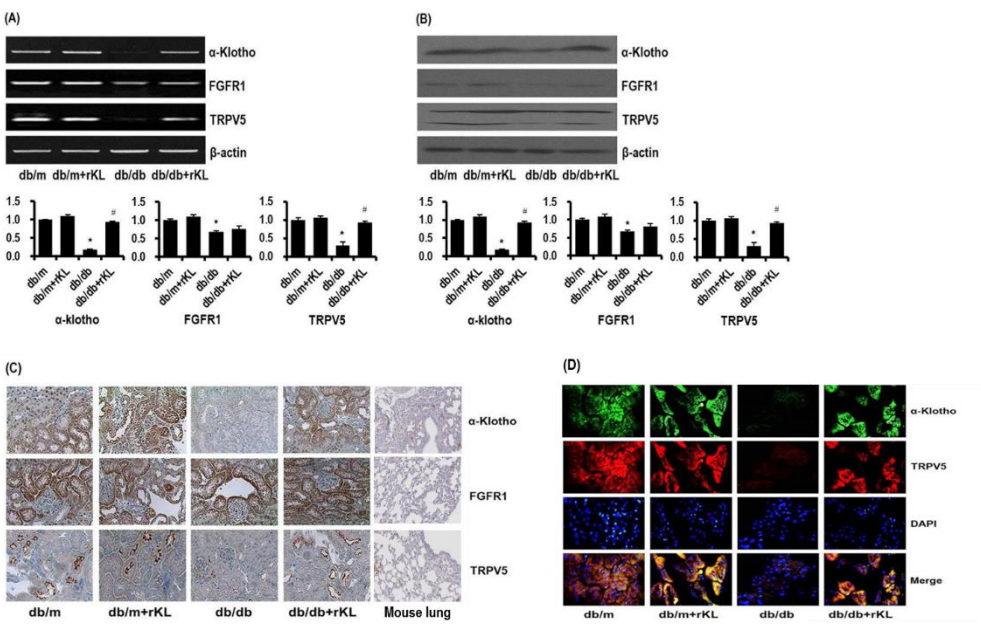

Figure 4.4. rKL increased renal α-klotho, FGFR1, and TRPV5 levels in db/db mice. (A) Genetic levels analyzed by PCR. (B) Renal protein expression analyzed

via western blot. (C) Protein expression analyzed by immunohistochemistry. Mice lung is used as negative control. (D) Tissue protein expression compared through immunofluorescence using a mouse kidney (magnification X 200).

4.3.5. Upregulation of renal TRPV5 by rKL in FGFR1-dependent and independent manners

As mentioned above, αklotho has two forms: membrane and soluble klotho. The full-length membrane αklotho is anchored on the membrane, binds with FGFR1, and functions as a co-receptor for FGF23[5]. To determine whether soluble αklotho increases TRPV5 in distal tubular cells, we performed an *in vitro* study using mouse distal tubular cells. Similar to the *in vivo experiment*, the expressions of αklotho, TRPV5, and FGFR1 were decreased when cells were exposed to high glucose (HG). When we administered rKL to cultured mDT, it also enhanced *klotho* expression under HG conditions (Figure 4.5A), and therefore it is likely to also increase membrane αklotho. Figure 4.5C shows that phosphorylation of molecules involved in FGF23 signaling, such as ERK and SGK[73], was suppressed

under HG conditions, but up-regulated by rKL treatment, indicating that rKL treatment also induced FGF23-FGFR1 signaling, which is a well-known pathway that increases TRPV5.

Next, we sought to determine whether rKL increases TRPV5 under HG conditions when FGF23 signaling is inhibited. To accomplish this, we inhibited FGFR1 by administering its inhibitor AZD4547[74] to mDT. rKL successfully increased TRPV5 in mDT under HG conditions even when FGFR1 was inhibited (Figure 4.5D). These observations confirm that soluble αklotho increases TRPV5 in both FGF23-dependent and FGF23-independent manners.

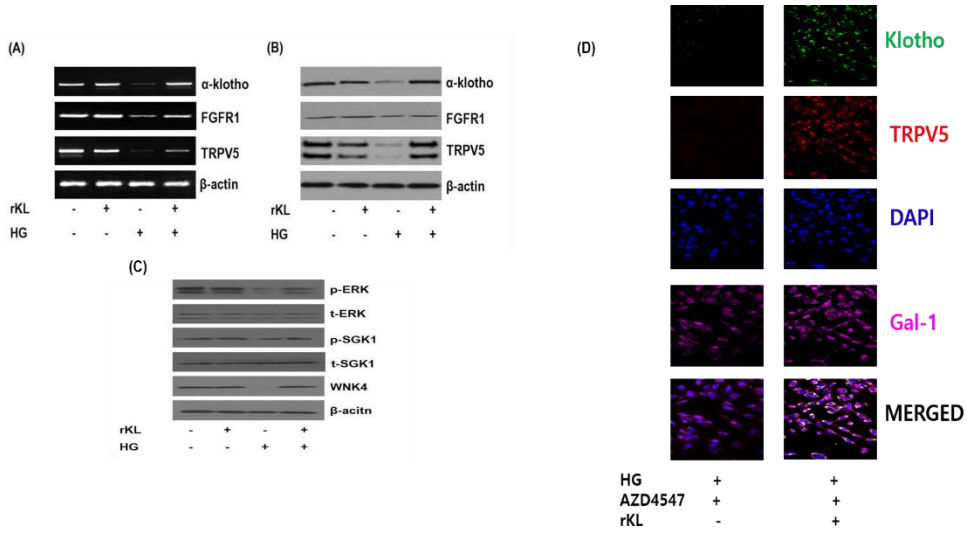

Figure 4.5. rKL increases TRPV5 on distal tubular cells through both FGF23-dependent and FGF23-independent mechanisms. (A) Genetic level analyzed by PCR. (B) Protein expression compared by western blot. (C) Molecules involved in FGF23-FGFR1, such as SGK, ERK, and WNT, are activated by rKL under HG conditions. (D) When FGFR1 is inhibited by AZD4547, rKL still increases TRPV5 under HG conditions (magnification X 200).

4.3.6. Soluble klotho binds to both TRPV5 and galectin 1

As previously mentioned, soluble klotho binds to TRPV5 though α2-3-sialyllactose[69]. Given that soluble rKL also upregulates TRPV5 in an FGF23-independent manner, we hypothesized that rKL binds to both TRPV5 and galectin 1. We performed *in vitro* immunofluorescence (IF) for αklotho, TRPV5, and galectin 1 using mDT in order to visualize whether they are all co-localized. As expected, IF showed co-localization of α-

klotho, TRPV5, and galectin-1, thereby confirming that the three molecules are co-localized in the cell. (Figure 4.6)

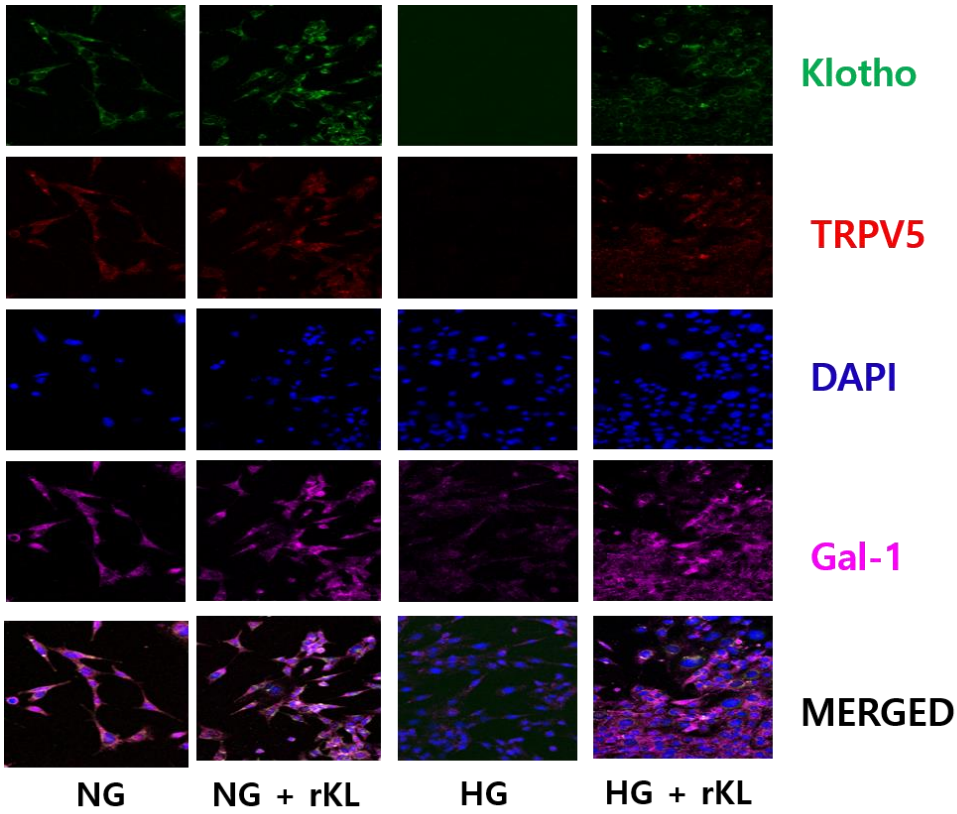

Figure 4.6. rKL binds to both TRPV5 and galecin-1.

4.3.7. rKL failed to up-regulate TRPV5 in distal tubular cells when both FGFR1 and galectin1 were inhibited

Since rKL increases TRPV5 under HG conditions without FGF23 signaling, and since it binds to galectin-1, we hypothesized that TRPV5 upregulation by soluble rKL without FGFR1 is galectin-1 dependent. Thus, we repeated the *in vitro* experiment using mDT with AZD4547 and galectin-1 inhibitor OTX008 to completely block the effects of rKL. When FGFR1 and galectin-1 were both inhibited, rKL did not up-regulate TRPV5 under both NG and HG conditions (Figure 4.7A). Immunofluorescence showed that even though αklotho is increased by rKL treatment, TRPV5 expression did not increase when both FGFR1 and galectin-1 were inhibited (Figure 4.7B). This drove us to conclude that sKL holds TRPV5 to the apical membrane of the renal distal tubule independent of FGF23, but in a galectin-1 dependent manner.

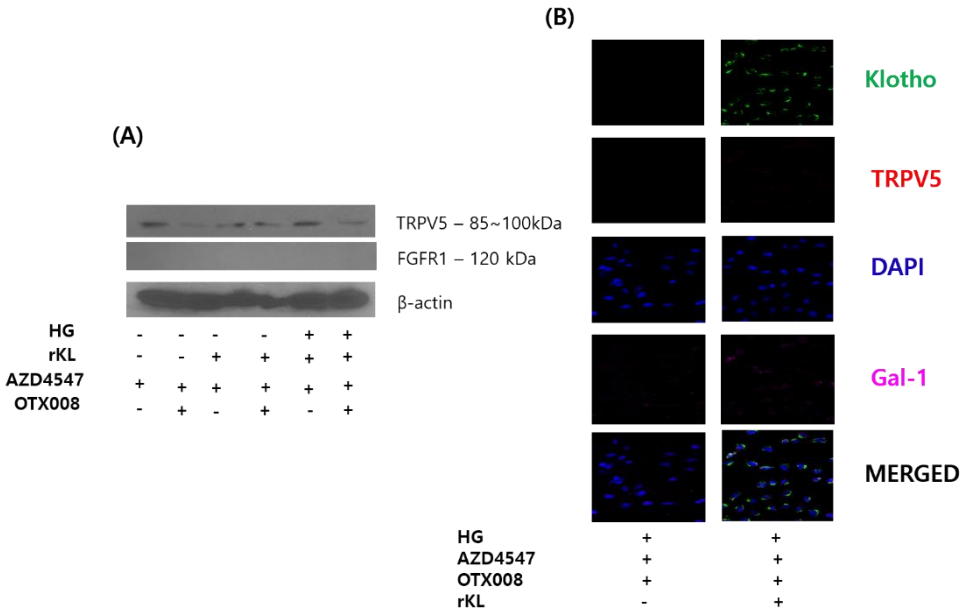

Figure 4.7. rKL could not increase TRPV5 when FGFR1 and galectin-1 were both inhibited. (A) Protein level analysis of *in vitro* results by western blot. (B) Protein expression analyzed by immunofluorescence (magnification X 200).

4.4 Discussion

α-Klotho increases TRPV5, thereby inducing renal calcium reabsorption[75]. The two forms of α-klotho, membrane and soluble α-klotho, increase TRPV5 through separate mechanisms. While membrane α-klotho induces TRPV5 expression and exocytosis in an FGF23-dependent manner, soluble α-klotho inhibits endocytosis of the membrane TRPV5 by bridging

TRPV5 with galectin-1, thereby tethering TRPV5 on the apical membrane. We uncovered the mechanism by which soluble α-klotho enhances TRPV5, independent of FGF23, as well as demonstrated that α-klotho is an important factor in the regulation of renal calcium excretion.

In the present study, we first observed that hypercalciuria occurs in db/db mice. We subsequently found that α-klotho, TRPV5, and FGFR1 are diminished in db/db mice and HG-exposed mDT cells, resulting in the introduction of these changes as the molecular mechanism for excessive urinary calcium excretion. Treatment of rKL enhanced TRPV5 both *in vivo* and *in vitro*, resulting in ameliorated hypercalciuria in db/db mice. We also observed the co-localization of KL, TRPV5, and galectin-1 together, which holds the transporter on the membrane, independent of FGF23 signaling. Given that soluble α-klotho binds to TRPV5 through α2-3-sialyllactose, we suggested that rKL might also possess a binding site to galectin-1 (Figure 8). We further proved this hypothesis by inhibiting galectin-1 and FGFR1 simultaneously, completely blocking the action of rKL to increase TRPV5 under HG conditions. We concluded that rKL increases TRPV5 not only through FGF23-FGFR1 signaling, but by tethering TRPV5 with galectin 1.

A recent study identified that soluble rKL binds to α2-3-sialyllactose through KL1 with a much higher affinity than through KL2. It showed that KL1 interacts with α2-3-sialyllactose much more favorably by ~10 kcal/mol than does KL2 and forms eight stable hydrogen bonds, whereas KL2 – α2-

3-sialyllactose complexes form only two hydrogen bonds [76]. Therefore, we suspect that rKL would bind galectin 1 through KL2. Moreover, the RBA domain is located in KL2, suggesting more molecules, possibly including galectin 1, can interact with rKL via KL2. Further studies based on the molecular structures are warranted to investigate whether KL2 includes a binding site for galectin-1.

In addition, soluble α-klotho increases the renal outer medullary potassium channel (ROMK)[77], and the mechanism appears identical to that of TRPV5 upregulation because ROMK also has α2-3-sialyllactose and binds to galectin-1 following treatment with α-klotho[68]. This suggests that α-klotho not only functions as the regulator of phosphorous but also of calcium and potassium homeostasis, further indicating that the intrinsically disordered structure of α-klotho has various functions still to be identified.

It is also likely that sKL may interact with many biological molecules, including α2-3-sialyllactose. In fact, a study reported that sKL targets α2-3-sialyllactose on monosialogangliosides, which are dynamically distributed on the cell membrane. The authors reported that sKL selectively binds to clustered α2-3-sialyllactose on lipid drafts, resulting in membrane structure alterations[78].

In a healthy kidney, about 60~70% of filtered calcium is reabsorbed in the proximal tubule. With no specific calcium transporter identified, calcium is believed to be reabsorbed passively in the proximal tubule as a result of reabsorption of sodium and water[79]. This inhibition of pharmacological

sodium-phosphate co-transporter 2a (Npt2a) was proven in a recent study using PF-06869206-induced calciuria in mice[80]. Although α-klotho also inhibits Napt2a in the proximal tubule via FGF23 signaling (which would inhibit passive calcium reabsorption), α-klotho also increases TRPV5 expression in the distal tubule, resulting in diminished Ca excretion as a whole in db/db mice. Our results indicate that TRPV5 is pivotal in renal calcium metabolism, and α-klotho may have complex effects on renal ion control beyond phosphorous metabolism.

We acknowledge that this study has several limitations. First, 6-week-old mice were too young to observe hypercalciuria-related disorders such as bone fracture, osteopenia, and nephrocalcinosis. Since we showed that rKL enhanced TRPV5 and therefore decreased Ca excretion in db/db mice, it is warranted to investigate the effect of long-term rKL treatment on diabetic mice in terms of bone-mineral metabolism. Second, 8 weeks of rKL treatment might not be long enough to observe a change in renal functions. This may explain why BUN and serum creatinine did not change in db/db mice. We believe that a longer period of treatment would have a different result, with a more significant change in BUN and serum creatinine. Besides, although db/db mice treated with rKL exhibited reduced Ca excretion, they showed lower serum calcium levels. Given that over 99 percent of total body calcium is stored in the bone, and only less than 1% of calcium is in circulation[81], serum calcium concentration may not necessarily represent the total body Ca store. Whether α-klotho induces

calcium entry into the bone needs further research. In fact, FGF23 is upregulated by parathyroid hormone (PTH)[82] and vitamin D[83], with PTH inducing calcium storage in the bone and vitamin D promoting calcium absorption in the intestine[84]. Since α-klotho functions as a co-receptor for FGF23, the role of α-klotho in calcium homeostasis is pivotal.

Taken together, we revealed the mechanism by which soluble α-klotho increases TRPV5 on the apical membrane of the renal distal tubule, independent of FGF23: soluble α-klotho anchors TRPV5 on the membrane via interactions with both TRPV5 and galectin-1.

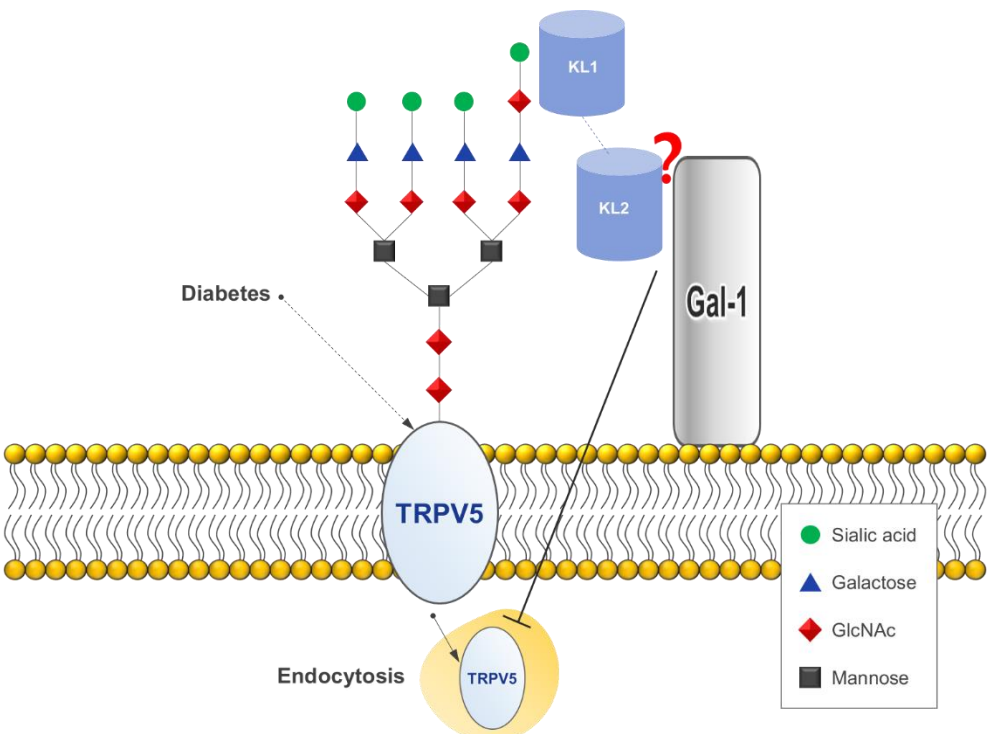

Figure 4.8. Soluble α-klotho inhibits diabetes-induced endocytosis of TRPV5 by anchoring it with galectin-1. While diabetes causes endocytosis and degradation of TRPV5, our study exhibited that soluble α-klotho inhibits this endocytosis by

binding with both TRPV5 (via α2-3-sialyllactose) and galectin-1, independent of FGF23. Since KL1 binds with α2-3-sialyllactose, the galectin-1 binding site in soluble α-klotho is likely to be located in KL2 (indicated by a question mark).

Chapter 5. General discussion and conclusion

DN is featured with decreased renal αklotho expression, and shows renal cell damage, including glomerular and tubular cells. αklotho is proven to show renal protective roles beyond inducing FGF23 signaling, but the exact function remains unknown. This study discovers that αklotho possesses protective roles against DN-mediated renal cell damage, suggesting that αklotho could be powerful treatment against DN.

In podocytes, αklotho suppressed TRPC6 overexpression, thereby protected podocytes and glomerular injury in db/db mice. This study found that αklotho diminished albuminuria, recovered glomerulus, and suppressed TRPC6 in db/db mice. Also, αklotho improved podocyte survivability and enhance synaptopodin in high glucose condition *in vitro*, by decreasing TRPC6, intracellular calcium concentration.

In renal proximal tubule, αklotho activated AMPK-PGC1α pathway, resulted in protected mitochondria in db/db mice. The second study showed that αklotho prevented mitochondrial damage in diabetic mice by increasing AMPK-PGC1α pathway, and renal NAD+. *in vitro,* αklotho protected

mitochondria and improved OXPHOS metabolism in S1 proximal tubule cells by increasing AMPK and PGC1α.

The third study discovered the new mechanism how soluble αklotho increased TRPV5 on renal distal tubule. The study reported that αklotho binds to both TRPV5 via α2-3-sialyllactos, and membrane protein galectin-1 simultaneously, thereby anchors TRPV5, and prevents its endocytosis mediated by DN. In db/db mice, αklotho diminished calcinuria and enhanced renal TRPV5. In cultured distal tubule cells, high glucose decreased TRPV5, and such decrease was inhibited by αklotho. Moreover, αklotho was found bound to both TRPV5 and galectin-1, and αklotho failed to increase TRPV5 when galectin-1 was inhibited.

Taken together, the studies conclude that an anti-ageing protein αklotho could act as a powerful regent against DN, which protects not only glomerulus, but also renal tubule. Future studies may include discovering additional beneficial functions that lurk in αklotho, and how deeply ageing and diabetes are related.

Reference

[1] M.C. Thomas, A.J. Weekes, O.J. Broadley, M.E. Cooper, T.H. Mathew, The burden of chronic kidney disease in Australian patients with type 2 diabetes (the NEFRON study), Med J Aust 185 (2006) 140-144.

[2] J.P. Dwyer, H.H. Parving, L.G. Hunsicker, M. Ravid, G. Remuzzi, J.B. Lewis, Renal Dysfunction in the Presence of Normoalbuminuria in Type 2 Diabetes: Results from the DEMAND Study, Cardiorenal Med 2 (2012) 1-10. 10.1159/000333249.

[3] A.J. Collins, R.N. Foley, B. Chavers, D. Gilbertson, C. Herzog, A. Ishani, K. Johansen, B.L. Kasiske, N. Kutner, J. Liu, W. St Peter, H. Guo, Y. Hu, A. Kats, S. Li, S. Li, J. Maloney, T. Roberts, M. Skeans, J. Snyder, C. Solid, B. Thompson, E. Weinhandl, H. Xiong, A. Yusuf, D. Zaun, C. Arko, S.C. Chen, F. Daniels, J. Ebben, E. Frazier, R. Johnson, D. Sheets, X. Wang, B. Forrest, D. Berrini, E. Constantini, S. Everson, P. Eggers, L. Agodoa, US Renal Data System 2013 Annual Data Report, Am J Kidney Dis 63 (2014) A7. 10.1053/j.ajkd.2013.11.001.

[4] S.A. Li, M. Watanabe, H. Yamada, A. Nagai, M. Kinuta, K. Takei, Immunohistochemical localization of Klotho protein in brain, kidney, and reproductive organs of mice, Cell Struct Funct 29 (2004) 91-99. 10.1247/csf.29.91.

[5] H. Kurosu, Y. Ogawa, M. Miyoshi, M. Yamamoto, A. Nandi, K.P. Rosenblatt, M.G. Baum, S. Schiavi, M.C. Hu, O.W. Moe, M. Kuro-o, Regulation of fibroblast growth factor-23 signaling by klotho, J Biol Chem 281 (2006) 6120-6123. 10.1074/jbc.C500457200.

[6] H. Murer, I. Forster, J. Biber, The sodium phosphate cotransporter family SLC34, Pflugers Arch 447 (2004) 763-767. 10.1007/s00424-003-1072-5.

[7] A. Imura, A. Iwano, O. Tohyama, Y. Tsuji, K. Nozaki, N. Hashimoto, T. Fujimori, Y. Nabeshima, Secreted Klotho protein in sera and CSF: implication for post-translational cleavage in release of Klotho protein from cell membrane, FEBS Lett 565 (2004) 143-147. 10.1016/j.febslet.2004.03.090.

[8] C.D. Chen, T.Y. Tung, J. Liang, E. Zeldich, T.B. Tucker Zhou, B.E. Turk, C.R. Abraham, Identification of cleavage sites leading to the shed form of the anti-aging protein klotho, Biochemistry 53 (2014) 5579-5587. 10.1021/bi500409n.

[9] M.C. Hu, K. Shiizaki, M. Kuro-o, O.W. Moe, Fibroblast growth factor 23 and Klotho: physiology and pathophysiology of an endocrine network of mineral metabolism, Annu Rev Physiol 75 (2013) 503-533. 10.1146/annurev-physiol-030212-183727.
[10] M.C. Hu, M. Kuro-o, O.W. Moe, The emerging role of Klotho in clinical nephrology, Nephrol Dial Transplant 27 (2012) 2650-2657. 10.1093/ndt/gfs160.
[11] G. Chen, Y. Liu, R. Goetz, L. Fu, S. Jayaraman, M.C. Hu, O.W. Moe, G. Liang, X. Li, M. Mohammadi, alpha-Klotho is a non-enzymatic molecular scaffold for FGF23 hormone signalling, Nature 553 (2018) 461-466. 10.1038/nature25451.
[12] S. Lee, J. Choi, J. Mohanty, L.P. Sousa, F. Tome, E. Pardon, J. Steyaert, M.A. Lemmon, I. Lax, J. Schlessinger, Structures of beta-klotho reveal a 'zip code'-like mechanism for endocrine FGF signalling, Nature 553 (2018) 501-505. 10.1038/nature25010.
[13] M.C. Hu, M. Shi, J. Zhang, H. Quinones, C. Griffith, M. Kuro-o, O.W. Moe, Klotho deficiency causes vascular calcification in chronic kidney disease, J Am Soc Nephrol 22 (2011) 124-136. 10.1681/ASN.2009121311.
[14] M.C. Hu, M. Shi, H.J. Cho, J. Zhang, A. Pavlenco, S. Liu, S. Sidhu, L.J. Huang, O.W. Moe, The erythropoietin receptor is a downstream effector of Klotho-induced cytoprotection, Kidney Int 84 (2013) 468-481. 10.1038/ki.2013.149.
[15] S.J. Shankland, The podocyte's response to injury: role in proteinuria and glomerulosclerosis, Kidney Int 69 (2006) 2131-2147. 10.1038/sj.ki.5000410.
[16] R. Nitschke, A. Henger, S. Ricken, J. Gloy, V. Muller, R. Greger, H. Pavenstadt, Angiotensin II increases the intracellular calcium activity in podocytes of the intact glomerulus, Kidney Int 57 (2000) 41-49. 10.1046/j.1523-1755.2000.00810.x.
[17] R. Sonneveld, J. van der Vlag, M.P. Baltissen, S.A. Verkaart, J.F. Wetzels, J.H. Berden, J.G. Hoenderop, T. Nijenhuis, Glucose specifically regulates TRPC6 expression in the podocyte in an AngII-dependent manner, Am J Pathol 184 (2014) 1715-1726. 10.1016/j.ajpath.2014.02.008.
[18] D.V. Ilatovskaya, O. Palygin, V. Chubinskiy-Nadezhdin, Y.A. Negulyaev, R. Ma, L. Birnbaumer, A. Staruschenko, Angiotensin II has acute effects on TRPC6 channels in podocytes of freshly isolated glomeruli, Kidney Int 86 (2014) 506-514. 10.1038/ki.2014.71.

[19] A. Whaley-Connell, J. Habibi, R. Nistala, S.A. Cooper, P.R. Karuparthi, M.R. Hayden, N. Rehmer, V.G. DeMarco, B.T. Andresen, Y. Wei, C. Ferrario, J.R. Sowers, Attenuation of NADPH oxidase activation and glomerular filtration barrier remodeling with statin treatment, Hypertension 51 (2008) 474-480. 10.1161/HYPERTENSIONAHA.107.102467.
[20] C. Faul, M. Donnelly, S. Merscher-Gomez, Y.H. Chang, S. Franz, J. Delfgaauw, J.M. Chang, H.Y. Choi, K.N. Campbell, K. Kim, J. Reiser, P. Mundel, The actin cytoskeleton of kidney podocytes is a direct target of the antiproteinuric effect of cyclosporine A, Nat Med 14 (2008) 931-938. 10.1038/nm.1857.
[21] J. Reiser, K.R. Polu, C.C. Moller, P. Kenlan, M.M. Altintas, C. Wei, C. Faul, S. Herbert, I. Villegas, C. Avila-Casado, M. McGee, H. Sugimoto, D. Brown, R. Kalluri, P. Mundel, P.L. Smith, D.E. Clapham, M.R. Pollak, TRPC6 is a glomerular slit diaphragm-associated channel required for normal renal function, Nat Genet 37 (2005) 739-744. 10.1038/ng1592.
[22] M.P. Winn, P.J. Conlon, K.L. Lynn, M.K. Farrington, T. Creazzo, A.F. Hawkins, N. Daskalakis, S.Y. Kwan, S. Ebersviller, J.L. Burchette, M.A. Pericak-Vance, D.N. Howell, J.M. Vance, P.B. Rosenberg, A mutation in the TRPC6 cation channel causes familial focal segmental glomerulosclerosis, Science 308 (2005) 1801-1804. 10.1126/science.1106215.
[23] S. Santin, E. Ars, S. Rossetti, E. Salido, I. Silva, R. Garcia-Maset, I. Gimenez, P. Ruiz, S. Mendizabal, J. Luciano Nieto, A. Pena, J.A. Camacho, G. Fraga, M.A. Cobo, C. Bernis, A. Ortiz, A.L. de Pablos, A. Sanchez-Moreno, G. Pintos, E. Mirapeix, P. Fernandez-Llama, J. Ballarin, R. Torra, F.S. Group, I. Zamora, J. Lopez-Hellin, A. Madrid, C. Ventura, R. Vilalta, L. Espinosa, C. Garcia, M. Melgosa, M. Navarro, A. Gimenez, J.V. Cots, S. Alexandra, C. Caramelo, J. Egido, M.D. San Jose, F. de la Cerda, P. Sala, F. Raspall, A. Vila, A.M. Daza, M. Vazquez, J.L. Ecija, M. Espinosa, M.L. Justa, R. Poveda, C. Aparicio, J. Rosell, R. Muley, J. Montenegro, D. Gonzalez, E. Hidalgo, D.B. de Frutos, E. Trillo, S. Gracia, F.J. de los Rios, TRPC6 mutational analysis in a large cohort of patients with focal segmental glomerulosclerosis, Nephrol Dial Transplant 24 (2009) 3089-3096. 10.1093/ndt/gfp229.
[24] C.C. Moller, C. Wei, M.M. Altintas, J. Li, A. Greka, T. Ohse, J.W. Pippin, M.P. Rastaldi, S. Wawersik, S. Schiavi, A. Henger, M. Kretzler, S.J. Shankland, J. Reiser,

Induction of TRPC6 channel in acquired forms of proteinuric kidney disease, J Am Soc Nephrol 18 (2007) 29-36. 10.1681/ASN.2006091010.
[25] J.H. Kim, J. Xie, K.H. Hwang, Y.L. Wu, N. Oliver, M. Eom, K.S. Park, N. Barrezueta, I.D. Kong, R.P. Fracasso, C.L. Huang, S.K. Cha, Klotho May Ameliorate Proteinuria by Targeting TRPC6 Channels in Podocytes, J Am Soc Nephrol 28 (2017) 140-151. 10.1681/ASN.2015080888.
[26] L.K. Farmer, R. Rollason, D.J. Whitcomb, L. Ni, A. Goodliff, A.C. Lay, L. Birnbaumer, K.J. Heesom, S.Z. Xu, M.A. Saleem, G.I. Welsh, TRPC6 Binds to and Activates Calpain, Independent of Its Channel Activity, and Regulates Podocyte Cytoskeleton, Cell Adhesion, and Motility, J Am Soc Nephrol 30 (2019) 1910-1924. 10.1681/ASN.2018070729.
[27] J. Xie, J. Yoon, S.W. An, M. Kuro-o, C.L. Huang, Soluble Klotho Protects against Uremic Cardiomyopathy Independently of Fibroblast Growth Factor 23 and Phosphate, J Am Soc Nephrol 26 (2015) 1150-1160. 10.1681/ASN.2014040325.
[28] H. Rakugi, N. Matsukawa, K. Ishikawa, J. Yang, M. Imai, M. Ikushima, Y. Maekawa, I. Kida, J. Miyazaki, T. Ogihara, Anti-oxidative effect of Klotho on endothelial cells through cAMP activation, Endocrine 31 (2007) 82-87. 10.1007/s12020-007-0016-9.
[29] J. Krtil, J. Platenik, M. Kazderova, V. Tesar, T. Zima, Culture methods of glomerular podocytes, Kidney Blood Press Res 30 (2007) 162-174. 10.1159/000102520.
[30] T. Inoguchi, P. Li, F. Umeda, H.Y. Yu, M. Kakimoto, M. Imamura, T. Aoki, T. Etoh, T. Hashimoto, M. Naruse, H. Sano, H. Utsumi, H. Nawata, High glucose level and free fatty acid stimulate reactive oxygen species production through protein kinase C--dependent activation of NAD(P)H oxidase in cultured vascular cells, Diabetes 49 (2000) 1939-1945. 10.2337/diabetes.49.11.1939.
[31] S.W. Schaffer, C.J. Jong, M. Mozaffari, Role of oxidative stress in diabetes-mediated vascular dysfunction: unifying hypothesis of diabetes revisited, Vascul Pharmacol 57 (2012) 139-149. 10.1016/j.vph.2012.03.005.
[32] M. Brownlee, Biochemistry and molecular cell biology of diabetic complications, Nature 414 (2001) 813-820. 10.1038/414813a.
[33] C. Canto, L.Q. Jiang, A.S. Deshmukh, C. Mataki, A. Coste, M. Lagouge, J.R. Zierath, J. Auwerx, Interdependence of AMPK and SIRT1 for metabolic adaptation

to fasting and exercise in skeletal muscle, Cell Metab 11 (2010) 213-219. 10.1016/j.cmet.2010.02.006.
[34] C. Canto, Z. Gerhart-Hines, J.N. Feige, M. Lagouge, L. Noriega, J.C. Milne, P.J. Elliott, P. Puigserver, J. Auwerx, AMPK regulates energy expenditure by modulating NAD+ metabolism and SIRT1 activity, Nature 458 (2009) 1056-1060. 10.1038/nature07813.
[35] J. Lin, H. Wu, P.T. Tarr, C.Y. Zhang, Z. Wu, O. Boss, L.F. Michael, P. Puigserver, E. Isotani, E.N. Olson, B.B. Lowell, R. Bassel-Duby, B.M. Spiegelman, Transcriptional co-activator PGC-1 alpha drives the formation of slow-twitch muscle fibres, Nature 418 (2002) 797-801. 10.1038/nature00904.
[36] D.J. Pagliarini, S.E. Calvo, B. Chang, S.A. Sheth, S.B. Vafai, S.E. Ong, G.A. Walford, C. Sugiana, A. Boneh, W.K. Chen, D.E. Hill, M. Vidal, J.G. Evans, D.R. Thorburn, S.A. Carr, V.K. Mootha, A mitochondrial protein compendium elucidates complex I disease biology, Cell 134 (2008) 112-123. 10.1016/j.cell.2008.06.016.
[37] S.P. Soltoff, ATP and the regulation of renal cell function, Annu Rev Physiol 48 (1986) 9-31. 10.1146/annurev.ph.48.030186.000301.
[38] L.J. Mandel, R.S. Balaban, Stoichiometry and coupling of active transport to oxidative metabolism in epithelial tissues, Am J Physiol 240 (1981) F357-371. 10.1152/ajprenal.1981.240.5.F357.
[39] M.C. Panesso, M. Shi, H.J. Cho, J. Paek, J. Ye, O.W. Moe, M.C. Hu, Klotho has dual protective effects on cisplatin-induced acute kidney injury, Kidney Int 85 (2014) 855-870. 10.1038/ki.2013.489.
[40] X. Xu, X. Tan, B. Tampe, T. Wilhelmi, M.S. Hulshoff, S. Saito, T. Moser, R. Kalluri, G. Hasenfuss, E.M. Zeisberg, M. Zeisberg, High-fidelity CRISPR/Cas9- based gene-specific hydroxymethylation rescues gene expression and attenuates renal fibrosis, Nat Commun 9 (2018) 3509. 10.1038/s41467-018-05766-5.
[41] K. Sharma, B. Karl, A.V. Mathew, J.A. Gangoiti, C.L. Wassel, R. Saito, M. Pu, S. Sharma, Y.H. You, L. Wang, M. Diamond-Stanic, M.T. Lindenmeyer, C. Forsblom, W. Wu, J.H. Ix, T. Ideker, J.B. Kopp, S.K. Nigam, C.D. Cohen, P.H. Groop, B.A. Barshop, L. Natarajan, W.L. Nyhan, R.K. Naviaux, Metabolomics reveals signature of mitochondrial dysfunction in diabetic kidney disease, J Am Soc Nephrol 24 (2013) 1901-1912. 10.1681/ASN.2013020126.

[42] E.F. Fang, S. Lautrup, Y. Hou, T.G. Demarest, D.L. Croteau, M.P. Mattson, V.A. Bohr, NAD(+) in Aging: Molecular Mechanisms and Translational Implications, Trends Mol Med 23 (2017) 899-916. 10.1016/j.molmed.2017.08.001.
[43] H. Bulluck, D.J. Hausenloy, Modulating NAD(+) metabolism to prevent acute kidney injury, Nat Med 24 (2018) 1306-1307. 10.1038/s41591-018-0181-9.
[44] P.R. Gavine, L. Mooney, E. Kilgour, A.P. Thomas, K. Al-Kadhimi, S. Beck, C. Rooney, T. Coleman, D. Baker, M.J. Mellor, A.N. Brooks, T. Klinowska, AZD4547: an orally bioavailable, potent, and selective inhibitor of the fibroblast growth factor receptor tyrosine kinase family, Cancer Res 72 (2012) 2045-2056. 10.1158/0008-5472.CAN-11-3034.
[45] A. Woods, S.R. Johnstone, K. Dickerson, F.C. Leiper, L.G. Fryer, D. Neumann, U. Schlattner, T. Wallimann, M. Carlson, D. Carling, LKB1 is the upstream kinase in the AMP-activated protein kinase cascade, Curr Biol 13 (2003) 2004-2008. 10.1016/j.cub.2003.10.031.
[46] M. Zhan, C. Brooks, F. Liu, L. Sun, Z. Dong, Mitochondrial dynamics: regulatory mechanisms and emerging role in renal pathophysiology, Kidney Int 83 (2013) 568-581. 10.1038/ki.2012.441.
[47] W.J. Liu, L. Ye, W.F. Huang, L.J. Guo, Z.G. Xu, H.L. Wu, C. Yang, H.F. Liu, p62 links the autophagy pathway and the ubiqutin-proteasome system upon ubiquitinated protein degradation, Cell Mol Biol Lett 21 (2016) 29. 10.1186/s11658-016-0031-z.
[48] A. Mullard, Anti-ageing pipeline starts to mature, Nat Rev Drug Discov 17 (2018) 609-612. 10.1038/nrd.2018.134.
[49] L.L. Dugan, Y.H. You, S.S. Ali, M. Diamond-Stanic, S. Miyamoto, A.E. DeCleves, A. Andreyev, T. Quach, S. Ly, G. Shekhtman, W. Nguyen, A. Chepetan, T.P. Le, L. Wang, M. Xu, K.P. Paik, A. Fogo, B. Viollet, A. Murphy, F. Brosius, R.K. Naviaux, K. Sharma, AMPK dysregulation promotes diabetes-related reduction of superoxide and mitochondrial function, J Clin Invest 123 (2013) 4888-4899. 10.1172/JCI66218.
[50] A. Salminen, K. Kaarniranta, AMP-activated protein kinase (AMPK) controls the aging process via an integrated signaling network, Ageing Res Rev 11 (2012) 230-241. 10.1016/j.arr.2011.12.005.
[51] E. Katsyuba, A. Mottis, M. Zietak, F. De Franco, V. van der Velpen, K. Gariani, D. Ryu, L. Cialabrini, O. Matilainen, P. Liscio, N. Giacche, N. Stokar-Regenscheit, D.

Legouis, S. de Seigneux, J. Ivanisevic, N. Raffaelli, K. Schoonjans, R. Pellicciari, J. Auwerx, De novo NAD(+) synthesis enhances mitochondrial function and improves health, Nature 563 (2018) 354-359. 10.1038/s41586-018-0645-6.
[52] H. Amano, A. Chaudhury, C. Rodriguez-Aguayo, L. Lu, V. Akhanov, A. Catic, Y.V. Popov, E. Verdin, H. Johnson, F. Stossi, D.A. Sinclair, E. Nakamaru-Ogiso, G. Lopez-Berestein, J.T. Chang, J.R. Neilson, A. Meeker, M. Finegold, J.A. Baur, E. Sahin, Telomere Dysfunction Induces Sirtuin Repression that Drives Telomere-Dependent Disease, Cell Metab 29 (2019) 1274-1290 e1279. 10.1016/j.cmet.2019.03.001.
[53] S. Sakai, T. Yamamoto, Y. Takabatake, A. Takahashi, T. Namba-Hamano, S. Minami, R. Fujimura, H. Yonishi, J. Matsuda, A. Hesaka, I. Matsui, T. Matsusaka, F. Niimura, M. Yanagita, Y. Isaka, Proximal Tubule Autophagy Differs in Type 1 and 2 Diabetes, J Am Soc Nephrol 30 (2019) 929-945. 10.1681/ASN.2018100983.
[54] M. Shi, B. Flores, N. Gillings, A. Bian, H.J. Cho, S. Yan, Y. Liu, B. Levine, O.W. Moe, M.C. Hu, alphaKlotho Mitigates Progression of AKI to CKD through Activation of Autophagy, J Am Soc Nephrol 27 (2016) 2331-2345. 10.1681/ASN.2015060613.
[55] S.H. Han, L. Malaga-Dieguez, F. Chinga, H.M. Kang, J. Tao, K. Reidy, K. Susztak, Deletion of Lkb1 in Renal Tubular Epithelial Cells Leads to CKD by Altering Metabolism, J Am Soc Nephrol 27 (2016) 439-453. 10.1681/ASN.2014121181.
[56] H.K. Liao, F. Hatanaka, T. Araoka, P. Reddy, M.Z. Wu, Y. Sui, T. Yamauchi, M. Sakurai, D.D. O'Keefe, E. Nunez-Delicado, P. Guillen, J.M. Campistol, C.J. Wu, L.F. Lu, C.R. Esteban, J.C. Izpisua Belmonte, In Vivo Target Gene Activation via CRISPR/Cas9-Mediated Trans-epigenetic Modulation, Cell 171 (2017) 1495-1507 e1415. 10.1016/j.cell.2017.10.025.
[57] F.J. Amaro-Gahete, O.A. De-la, L. Jurado-Fasoli, A. Espuch-Oliver, T. de Haro, A. Gutierrez, J.R. Ruiz, M.J. Castillo, Exercise training increases the S-Klotho plasma levels in sedentary middle-aged adults: A randomised controlled trial. The FIT-AGEING study, J Sports Sci 37 (2019) 2175-2183. 10.1080/02640414.2019.1626048.
[58] P. Raskin, M.R. Stevenson, D.E. Barilla, C.Y. Pak, The hypercalciuria of diabetes mellitus: its amelioration with insulin, Clin Endocrinol (Oxf) 9 (1978) 329-335. 10.1111/j.1365-2265.1978.tb02218.x.

[59] D.T. Ward, S.K. Yau, A.P. Mee, E.B. Mawer, C.A. Miller, H.O. Garland, D. Riccardi, Functional, molecular, and biochemical characterization of streptozotocin-induced diabetes, J Am Soc Nephrol 12 (2001) 779-790.
[60] O. Asai, K. Nakatani, T. Tanaka, H. Sakan, A. Imura, S. Yoshimoto, K. Samejima, Y. Yamaguchi, M. Matsui, Y. Akai, N. Konishi, M. Iwano, Y. Nabeshima, Y. Saito, Decreased renal alpha-Klotho expression in early diabetic nephropathy in humans and mice and its possible role in urinary calcium excretion, Kidney Int 81 (2012) 539-547. 10.1038/ki.2011.423.
[61] A. Imura, Y. Tsuji, M. Murata, R. Maeda, K. Kubota, A. Iwano, C. Obuse, K. Togashi, M. Tominaga, N. Kita, K. Tomiyama, J. Iijima, Y. Nabeshima, M. Fujioka, R. Asato, S. Tanaka, K. Kojima, J. Ito, K. Nozaki, N. Hashimoto, T. Ito, T. Nishio, T. Uchiyama, T. Fujimori, Y. Nabeshima, alpha-Klotho as a regulator of calcium homeostasis, Science 316 (2007) 1615-1618. 10.1126/science.1135901.
[62] M. Kuro-o, Y. Matsumura, H. Aizawa, H. Kawaguchi, T. Suga, T. Utsugi, Y. Ohyama, M. Kurabayashi, T. Kaname, E. Kume, H. Iwasaki, A. Iida, T. Shiraki-Iida, S. Nishikawa, R. Nagai, Y.I. Nabeshima, Mutation of the mouse klotho gene leads to a syndrome resembling ageing, Nature 390 (1997) 45-51. 10.1038/36285.
[63] L. Bloch, O. Sineshchekova, D. Reichenbach, K. Reiss, P. Saftig, M. Kuro-o, C. Kaether, Klotho is a substrate for alpha-, beta- and gamma-secretase, FEBS Lett 583 (2009) 3221-3224. 10.1016/j.febslet.2009.09.009.
[64] C.D. Chen, S. Podvin, E. Gillespie, S.E. Leeman, C.R. Abraham, Insulin stimulates the cleavage and release of the extracellular domain of Klotho by ADAM10 and ADAM17, Proc Natl Acad Sci U S A 104 (2007) 19796-19801. 10.1073/pnas.0709805104.
[65] M.C. Hu, M. Shi, J. Zhang, T. Addo, H.J. Cho, S.L. Barker, P. Ravikumar, N. Gillings, A. Bian, S.S. Sidhu, M. Kuro-o, O.W. Moe, Renal Production, Uptake, and Handling of Circulating alphaKlotho, J Am Soc Nephrol 27 (2016) 79-90. 10.1681/ASN.2014101030.
[66] S.K. Cha, B. Ortega, H. Kurosu, K.P. Rosenblatt, O.M. Kuro, C.L. Huang, Removal of sialic acid involving Klotho causes cell-surface retention of TRPV5 channel via binding to galectin-1, Proc Natl Acad Sci U S A 105 (2008) 9805-9810. 10.1073/pnas.0803223105.

[67] K. Ohtsubo, S. Takamatsu, M.T. Minowa, A. Yoshida, M. Takeuchi, J.D. Marth, Dietary and genetic control of glucose transporter 2 glycosylation promotes insulin secretion in suppressing diabetes, Cell 123 (2005) 1307-1321. 10.1016/j.cell.2005.09.041.
[68] E.A. Partridge, C. Le Roy, G.M. Di Guglielmo, J. Pawling, P. Cheung, M. Granovsky, I.R. Nabi, J.L. Wrana, J.W. Dennis, Regulation of cytokine receptors by Golgi N-glycan processing and endocytosis, Science 306 (2004) 120-124. 10.1126/science.1102109.
[69] J.D. Wright, S.W. An, J. Xie, J. Yoon, N. Nischan, J.J. Kohler, N. Oliver, C. Lim, C.L. Huang, Modeled structural basis for the recognition of alpha2-3-sialyllactose by soluble Klotho, FASEB J 31 (2017) 3574-3586. 10.1096/fj.201700043R.
[70] M. Azuma, D. Koyama, J. Kikuchi, H. Yoshizawa, D. Thasinas, K. Shiizaki, M. Kuro-o, Y. Furukawa, E. Kusano, Promoter methylation confers kidney-specific expression of the Klotho gene, FASEB J 26 (2012) 4264-4274. 10.1096/fj.12-211631.
[71] T. Arbel Rubinstein, S. Shahmoon, E. Zigmond, T. Etan, K. Merenbakh-Lamin, M. Pasmanik-Chor, G. Har-Zahav, I. Barshack, G.W. Vainer, N. Skalka, R. Rosin-Arbesfeld, C. Varol, T. Rubinek, I. Wolf, Klotho suppresses colorectal cancer through modulation of the unfolded protein response, Oncogene 38 (2019) 794-807. 10.1038/s41388-018-0489-4.
[72] J.H. Pizzonia, F.A. Gesek, S.M. Kennedy, B.A. Coutermarsh, B.J. Bacskai, P.A. Friedman, Immunomagnetic separation, primary culture, and characterization of cortical thick ascending limb plus distal convoluted tubule cells from mouse kidney, In Vitro Cell Dev Biol 27A (1991) 409-416. 10.1007/BF02630961.
[73] O. Andrukhova, U. Zeitz, R. Goetz, M. Mohammadi, B. Lanske, R.G. Erben, FGF23 acts directly on renal proximal tubules to induce phosphaturia through activation of the ERK1/2-SGK1 signaling pathway, Bone 51 (2012) 621-628. 10.1016/j.bone.2012.05.015.
[74] J. Kang, Y.J. Choi, B.Y. Seo, U. Jo, S.I. Park, Y.H. Kim, K.H. Park, A Selective FGFR inhibitor AZD4547 suppresses RANKL/M-CSF/OPG-dependent ostoclastogenesis and breast cancer growth in the metastatic bone microenvironment, Sci Rep 9 (2019) 8726. 10.1038/s41598-019-45278-w.
[75] O. Andrukhova, A. Smorodchenko, M. Egerbacher, C. Streicher, U. Zeitz, R. Goetz, V. Shalhoub, M. Mohammadi, E.E. Pohl, B. Lanske, R.G. Erben, FGF23

promotes renal calcium reabsorption through the TRPV5 channel, EMBO J 33 (2014) 229-246. 10.1002/embj.201284188.
[76] J.D. Wright, S.W. An, J. Xie, C. Lim, C.L. Huang, Soluble klotho regulates TRPC6 calcium signaling via lipid rafts, independent of the FGFR-FGF23 pathway, FASEB J 33 (2019) 9182-9193. 10.1096/fj.201900321R.
[77] S.K. Cha, M.C. Hu, H. Kurosu, M. Kuro-o, O. Moe, C.L. Huang, Regulation of renal outer medullary potassium channel and renal K(+) excretion by Klotho, Mol Pharmacol 76 (2009) 38-46. 10.1124/mol.109.055780.
[78] G. Dalton, S.W. An, S.I. Al-Juboori, N. Nischan, J. Yoon, E. Dobrinskikh, D.W. Hilgemann, J. Xie, K. Luby-Phelps, J.J. Kohler, L. Birnbaumer, C.L. Huang, Soluble klotho binds monosialoganglioside to regulate membrane microdomains and growth factor signaling, Proc Natl Acad Sci U S A 114 (2017) 752-757. 10.1073/pnas.1620301114.
[79] R.T. Alexander, H. Dimke, Effect of diuretics on renal tubular transport of calcium and magnesium, Am J Physiol Renal Physiol 312 (2017) F998-F1015. 10.1152/ajprenal.00032.2017.
[80] L. Thomas, J. Xue, S.K. Murali, R.A. Fenton, J.A. Dominguez Rieg, T. Rieg, Pharmacological Npt2a Inhibition Causes Phosphaturia and Reduces Plasma Phosphate in Mice with Normal and Reduced Kidney Function, J Am Soc Nephrol 30 (2019) 2128-2139. 10.1681/ASN.2018121250.
[81] A.C. Ross, The 2011 report on dietary reference intakes for calcium and vitamin D, Public Health Nutr 14 (2011) 938-939. 10.1017/S1368980011000565.
[82] V. Lavi-Moshayoff, G. Wasserman, T. Meir, J. Silver, T. Naveh-Many, PTH increases FGF23 gene expression and mediates the high-FGF23 levels of experimental kidney failure: a bone parathyroid feedback loop, Am J Physiol Renal Physiol 299 (2010) F882-889. 10.1152/ajprenal.00360.2010.
[83] T.K. Barthel, D.R. Mathern, G.K. Whitfield, C.A. Haussler, H.A.t. Hopper, J.C. Hsieh, S.A. Slater, G. Hsieh, M. Kaczmarska, P.W. Jurutka, O.I. Kolek, F.K. Ghishan, M.R. Haussler, 1,25-Dihydroxyvitamin D3/VDR-mediated induction of FGF23 as well as transcriptional control of other bone anabolic and catabolic genes that orchestrate the regulation of phosphate and calcium mineral metabolism, J Steroid Biochem Mol Biol 103 (2007) 381-388. 10.1016/j.jsbmb.2006.12.054.

[84] J.E.i.G.a.H.T.o.M. Hall, Physiology 13th edn 1001–1019 (Elsevier, Hall, J. E. in Guyton and Hall Textbook of Medical

Physiology 13th edn 1001–1019 (Elsevier, 2016). 2016.

요약 (국문초록)

당뇨병성 신증모델에서 항노화물질인 αklotho의 신기능 보호 효과

의학과 중개의학 전공

이진호

배경

당뇨병은 혈당의 급격한 증가로 인해 발생하며, 만성 콩팥병과 노화에도 큰 연관성을 가진다. 실제로 제 2형 당뇨병환자의 약 50%, 제 1형 당뇨병환자의 약 3분의 1이 신기능 저하와 단백뇨 현상을 보인다. 따라서, 미국에서는 당뇨병성 신증이 만성 신부전증의 주요 원인으로 자리매김하고 있다.

αklotho는 주로 신장에서 발현하는 항노화 물질이며, 당뇨병성 신증에 의해 그 발현량이 감소한다. αklotho는 신장내 세뇨관뿐 아니라 족세포에서도 그 발현이 관찰된다. αklotho의 가장 잘 알려진 기능으로는 섬유아세포 성장인자 23의 수용체로서, 인산뇨 배출을 유도하는 것이다. 하지만 가용성 형태의 αklotho가 혈류를 타고 흐른다는 점과, 다양한 다른 분자와 결합할 수 있다는 특징으로 인해 여러 기능이 있을 것으로 생각되어진다. 실제로 αklotho는 자식 작용

(autophagy), 상처회복, 항산화 작용, 인슐린 민감도증가 등에도 관련이 있다는 보고가 있다.

본 연구는 αklotho가 기존에 알려진 기능 외에 다른 기전으로 당뇨병성 신증 모델의 마우스에서 신기능 보호 효과가 있는지 연구하기위해 제 2형 당뇨병 모델인 db/db 마우스에 재조합 αklotho 단백질을 8주간 주사하였다. 그 결과 αklotho는 신장 족세포 (podocyte)에서 TRPC6의 과발현을 방지하여 족세포 밑 사구체 손상을 방지하여 단백뇨를 예방하였다. 뿐만 아니라 근위 세뇨관에서 αklotho는 AMPK-PGC1α을 증가시켜 db/db 마우스의 신장내 미토콘드리아가 보호되는 효과를 관찰하였다. 추가로 원위 세뇨관에서 αklotho가 TRPV5와 세포막 단백질인 galectin-1 과 동시결합함으로 인해 초기 당뇨병에서 발생하는 TRPV5 감소현상을 방지하고 칼슘뇨배출증가를 방지하는 기전을 새롭게 발견하였다. 이 연구들을 통해 항노화물질인 αklotho가 당뇨병성 신증모델에서 다양한 신기능 보호효과를 가진 물질임을 주장하고자 한다.

방법

제 2 형 당뇨병의 마우스 모델인 db/db 마우스 (수컷, 6 주령) 을 14 두 구입하여, 그중 7 두에 재조합 αklotho 단백질 (rKL) 을 8 주간, 10μg/kg 로 매일 복강주사하여, vehicle (saline) 을 주사한 남은 7 두의 db/db 마우스와 비교하였다. 또한 대조군으로 db/m 마우스 (수컷, 6 주령)을 14 두 구입하여, 그중 7 두에 rKL 을 주사했고, 남은 7 두는 saline 을 주사하였다. 추가로 당뇨와 다른 단백뇨 모델을 만들기 위해 PAN 을 주사할 마우스 7 두 (수컷, 7 주령) 구입하여 2 주에 1 회, 100mg/kg 로 복강주사 하였다. 모든 마우스는 주사기간 종료직후 metabolic cage 를 이용하여 24 시간 소변을 채취하였고, 이후 희생되었다. 희생직전 모든 마우스의 혈압, 혈당, 체중을 측정하였고, 희생직후 신장을 채취하였다.

In vitro 연구로는 마우스 S1 근위세뇨관 세포과 원위세뇨관 세포, 그리고 마우스의 족세포 (podocyte)를 이용하였다. 당뇨를 모방하기위해 30m 의 고농축 포도당 과 5mM 의 정상 포도당 처리군에서 rKL 처리/비처리군으로 나누어 24 시간 처리 후 각 분자의 발현량을 분석하였다.

결과

rKL 을 처리한 db/db 마우스에서는 saline 만을 처리한 대조군 db/db 그룹에 비해 1) TRPC6 의 현저한 감소, 사구체 손상의 감소, 칼슘뇨배출의 감소를 보였고, 2) 신장내 미코콘드리아 손상의 감소, AMPK-PGC1α 의 증가, 신장 내 NAD+ 의 증가를 보였으며, 3) 신장의 TRPV5 의 증가와 칼슘뇨배출의 현저한 감소를 보였다.

배양한 세포를 이용한 *in vitro* 연구에서는 rKL 을 처리한 고 포도당 군에서 대조군 고 포도당 군에 비해 4) 배양한 족세포에서 TRPC6 와 세포내 칼슘농도의 감소, 그리고 synaptopodin 의 증가와 족세포 생존률이 증가함을 확인하였고, 5) 근위세뇨관 세포에서의 미토콘드리아 회복 및 기능 증가, AMPK-PGC1α 의 증가를 확인 하였으며, 6) 원위세뇨관 세포에서의 TRPV5 증가와 αklotho, TRPV5, galectin-1 의 결합, 그리고 OTX008 로 galectin-1 을 억제하자 αklotho 가 TRPV5 를 증가시키지 못함을 확인하였다.

결론

재조합 αklotho(rKL)는 db/db 마우스에서 TRPC6 과발현 억제를 통해 사구체를 보호함으로써 단백뇨를 감소시켰고, LKB1 활성화를 통한 AMPK-PGC1α 을 증가시켜 근위세뇨관에서 미토콘드리아를 보호하였으며, 원위세뇨관에서는 TRPV5 와 galectin-1 과 동시결합하여 TRPV5 를 membrane 에 붙잡아 둠으로써 당뇨에서 발생하는 TRPV5 의 감소를 저해하여 칼슘뇨배출을 억제하였다. 본 연구의 결과는 αklotho 가 항 노화물질 뿐 아니라 항 당뇨성 물질로도 큰 도움이 될 수 있음을 시사한다.

주요어: αklotho, 당뇨병성 신증, 족세포, TRPC6, 근위 세뇨관, 미토콘드리아, AMPK-PGC1α, 원위 세뇨관, TRPV5, galectin-1

학번: 2016-20030